Circadian rhythms of macrophages are altered by the acidic pH of the tumor microenvironment.

Amelia M. Knudsen-Clark[1], Daniel Mwangi[2], Juliana Cazarin[2], Lauren M. Hablitz[3], Minsoo Kim[1], Brian J. Altman[2,4*].

[1]Department of Microbiology and Immunology, [2]Department of Biomedical Genetics, [3]Center for Translational Neuromedicine, and [4]Wilmot Cancer Institute, University of Rochester Medical Center, Rochester, New York, USA.

*Corresponding author.

E-mail: Brian_Altman@URMC.rochester.edu

Abstract

Macrophages are prime therapeutic targets due to their pro-tumorigenic and immunosuppressive functions in tumors, but varying efficacy of therapeutic approaches targeting macrophages highlights our incomplete understanding of how the tumor microenvironment (TME) can influence regulation of macrophages. The circadian clock is a key internal regulator of macrophage function, but how circadian rhythms of macrophages may be influenced by the tumor microenvironment remains unknown. We found that conditions associated with the TME such as polarizing stimuli, acidic pH, and elevated lactate concentrations can each alter circadian rhythms in macrophages. Circadian rhythms were enhanced in pro-resolution macrophages but suppressed in pro-inflammatory macrophages, while acidic pH had divergent effects on circadian rhythms depending on macrophage phenotype. While cyclic AMP (cAMP) has been reported to play a role in macrophage response to acidic pH, our results indicate that pH-driven changes in circadian rhythms are not mediated solely by the cAMP signaling pathway. Remarkably, clock

correlation distance analysis of tumor-associated macrophages (TAMs) revealed evidence of circadian disorder in TAMs. This is the first report providing evidence that circadian rhythms of macrophages are altered within the TME. Our data suggest that heterogeneity in circadian rhythms at the population level may underlie this circadian disorder. Finally, we sought to determine how circadian regulation of macrophages impacts tumorigenesis, and found that tumor growth was suppressed when macrophages had a functional circadian clock. Our work demonstrates a novel mechanism by which the tumor microenvironment can influence macrophage biology through altering circadian rhythms, and the contribution of circadian rhythms in macrophages to suppressing tumor growth.

37 # Introduction

38

39 Tumor-associated macrophages (TAMs) are one of the most abundant leukocytes found in solid tumors,
40 with high intra-tumoral TAM density generally associated with poor clinical outcome [1-3]. This is
41 consistent with the largely pro-tumorigenic role of macrophages within tumors[4]. Macrophages are
42 highly plastic professional phagocytes whose ability to sense and respond to the environment makes
43 them uniquely equipped to protect tissue integrity under normal homeostatic conditions[5, 6]. However,
44 within the chronically inflamed tumor microenvironment (TME), failure to resolve the inflammation can
45 lead to uncontrolled secretion of tissue repair factors by TAMs, promoting tumor growth and metastatic
46 capacity[7-9]. At the same time, conditions in the TME can drive TAMs to suppress potentially anti-
47 tumorigenic inflammatory activity through various mechanisms including secretion of anti-inflammatory
48 cytokines and expression of checkpoint inhibitors such as PD-L1, promoting immune suppression[4, 10-
49 16].

50

51 TAMs are known to suppress the response to many standard of care treatments through their pro-
52 tumorigenic and immunosuppressive functions, making them a prime therapeutic target[17]. However,
53 we still have an incomplete understanding of how the TME influences macrophages, limiting our ability
54 to target them; this is highlighted by the varying efficacy of therapeutic approaches used to target
55 macrophages[18]. This is thought to be due in part to the significant phenotypical heterogeneity of TAMs
56 within tumors[18-20]. Evidence suggests this heterogeneity is due to the ability of macrophages to sense
57 and adapt to the local microenvironment, which varies within tumors depending on several factors
58 including the distance from blood vessels and neighboring cells[21-24]. Indeed, various conditions in the
59 TME have been shown to influence macrophage phenotype and function[4].

60

61 In particular, poor vascularization of solid tumors leads to inefficient delivery of oxygen, creating regions
62 of hypoxia[25]. The hypoxic response promotes enhanced glycolytic activity of cells within the region,
63 which, coupled with poor tissue drainage as a result of leaky vasculature, results in elevated levels of
64 protons and lactate, acidifying the microenvironment[26, 27]. Of conditions in the TME, it has been well
65 appreciated that acidic pH can promote a pro-resolution phenotype, thereby contributing to the pro-
66 tumorigenic and immunosuppressive functions of macrophages within tumors[28-30].
67
68 The myriad ways in which the TME can impact regulation of macrophages remain to be fully elucidated.
69 Circadian rhythms are a key regulatory system that is present in almost all cells of the body, and are an
70 understudied facet of macrophage biology[31]. Acidic pH is a condition commonly associated with the
71 TME that has been shown to alter circadian rhythms in cell lines[32]; however, whether pH influences
72 circadian rhythms in macrophages remain unknown.
73
74 Circadian rhythms are 24-hour rhythms that impart oscillations in the levels of circadian-regulated gene
75 transcripts and proteins in a tissue- and cell-specific manner, resulting in time-of-day-dependent variation
76 in many cellular processes[33, 34]. The molecular clock, which we will refer to as the circadian clock, drives
77 these rhythms in cells through a cell-autonomous transcription/translation feedback loop, which is
78 controlled in part by the transcription factor BMAL1[31]. Circadian clocks are synchronized by signals sent
79 out from the central circadian clock housed within the suprachiasmatic nucleus of the hypothalamus,
80 which entrains circadian clocks to the time of day[31]. This allows for the temporal coordination of cells
81 in spatially distinct tissues, although how the local microenvironment influences circadian rhythms
82 remains to be elucidated.
83

84 All leukocytes tested to date have functional circadian clocks[35-42]. As such, nearly every arm of the
85 immune response (both innate and adaptive) is subject to circadian regulation[35, 37, 43]. Time-of-day-
86 dependent regulation of immune responses is achieved though temporal gating of response to stimuli,
87 effector function, and cell trafficking[42, 44-48], all of which promote coordination between the multiple
88 phases of the immune response[40, 42, 49-53].
89
90 Key aspects of macrophage function are subject to circadian regulation, including cytokine secretion and
91 phagocytosis[36, 44, 45, 51, 54]. This results in a time-of-day-dependent macrophage response to
92 stimuli, which modulates the magnitude of the resulting adaptive immune response and determines
93 disease progression[44, 51, 55]. Circadian regulation of macrophages is of particular interest given
94 recent evidence of time-of-day variation in the frequency of TAMs expressing surface markers associated
95 with phenotype[56-58]. A promising application of such circadian variation was made evident in
96 leveraging observations of circadian frequency in TAMs expressing immune checkpoint blockade (ICB)
97 target PD-1 to increase efficacy of PD-1/PD-L1 ICB therapy by timing treatment to the time of day when
98 PD-1+ TAMs were most frequent[57, 59]. This suggests that leveraging time-of-day variations in
99 therapeutic targets could be promising avenue to increase efficacy, highlighting the importance of
100 understanding how circadian rhythms of macrophages may be influenced by conditions in the TME,
101 which remains unclear.
102
103 In this work, we present evidence that circadian rhythms of macrophages are altered in the TME. We
104 uncover a novel way in which two conditions within the TME, acidic pH and lactate, can influence
105 macrophage biology through modulation of circadian rhythms. We also find that macrophages of
106 different phenotypes have distinct circadian rhythms. Remarkably, we found evidence of circadian
107 disorder in tumor-associated macrophages, indicating that circadian rhythms are altered in macrophages

108 within the TME. Furthermore, our data suggest that heterogeneity in circadian rhythms at the
109 population level may underlie the observed circadian disorder. This work elucidates a novel way in which
110 the TME can alter macrophage biology, and represents the first steps to understanding how the tumor
111 microenvironment can alter circadian rhythms of immune cells such as macrophages.
112

113 Results

114

115 **Macrophages of different phenotypes exhibit different circadian rhythms.**

116

117 As macrophages are a phenotypically heterogeneous population in the TME, we first sought to
118 understand whether diversity in macrophage phenotype could translate to diversity in circadian rhythms
119 of macrophages. To this end, we used the well-established *in vitro* polarization models of IL-4 and IL-13-
120 stimulated (pro-resolution, often referred to as 'M2' and used as a model of pro-tumorigenic
121 macrophages) and IFNγ and LPS-stimulated (pro-inflammatory, often referred to as 'M1' and broadly
122 viewed as anti-tumorigenic) macrophages. Arginase 1 (ARG1; *Arg1*) and Inducible Nitric Oxide Synthase
123 (iNOS; *Nos2*) are upregulated in pro-resolution and pro-inflammatory macrophages, respectively, and
124 thus are commonly used as markers of the pro-resolution or pro-inflammatory phenotype in
125 macrophages[60]. Consistent with previous studies, we found that *Arg1* was induced in IL-4 and IL-13-
126 stimulated macrophages, but not IFNγ and LPS-stimulated macrophages; in contrast, *Nos2* was induced
127 in IFNγ and LPS-stimulated macrophages, but not IL-4 and IL-13-stimulated macrophages
128 (Supplementary Figure 1). This indicates that macrophages stimulated with IL-4 and IL-13 were polarized
129 toward a pro-resolution phenotype, while macrophages stimulated with IFNγ and LPS were polarized
130 toward a pro-inflammatory phenotype.
131

132 Circadian rhythms of macrophages were measured by monitoring PER2, a key component of the
133 circadian clock, via the rhythmic activity of the PER2-Luciferase (PER2-Luc) fusion protein in a live cell
134 LumiCycle luminometer (Supplementary Figure 2A)[61]. Bone marrow-derived macrophages (BMDMs)
135 were generated from bone marrow of mice expressing PER2-Luc. Following differentiation, the circadian
136 clocks of BMDMs were synchronized, and rhythms were observed for up to 4 days (Figure 2B).
137
138 To determine whether phenotype can influence circadian rhythms in macrophages, BMDMs were
139 cultured in the presence or absence of polarizing stimuli, and rhythms were observed by LumiCycle
140 (Figure 1). The amplitude of rhythms is the magnitude of change between the peak and the trough, and
141 is indicative of the strength of rhythms[62, 63]. Amplitude of rhythms was suppressed in pro-
142 inflammatory macrophages compared to unstimulated macrophages. In contrast, amplitude of rhythms
143 in pro-resolution macrophages was enhanced. This suggests that rhythms are suppressed in pro-
144 inflammatory macrophages but enhanced in pro-resolution macrophages, which agrees with previous
145 observations[64, 65]. Period is the amount of time it takes to complete one full oscillation, and is
146 indicative of how fast the circadian clock is running[66]. Compared to unstimulated macrophages, period
147 was lengthened in pro-resolution macrophages but shortened in pro-inflammatory macrophages. This In
148 line with others' observations, and suggests that the clock runs slower in pro-resolution macrophages
149 but runs faster in pro-inflammatory macrophages[64, 65].
150
151 Interestingly, we observed differences in damping of rhythms in polarized macrophages. Damping is
152 measured as the number of days required for the amplitude of rhythms to decrease by 30% of the first
153 cycle[67]. Damping of rhythms in most free-running cell populations, cultured in the absence of external
154 synchronizing stimuli, occurs naturally as the circadian clocks of individual cells in the population become
155 desynchronized from each other; thus, damping can be indicative of desynchrony within a

population[68]. The damping rate increases as the number of days required for rhythms to damp decreases; conversely, as damping rate decreases as the number of days required for rhythms to damp increases. We observed increased rate of damping in pro-inflammatory macrophages compared to unstimulated macrophages, indicating that population-level rhythms were maintained for a shorter period of time in pro-inflammatory macrophages. In contrast, damping rate was decreased in pro-resolution macrophages, indicating that population-level rhythms were maintained for longer in pro-resolution macrophages. These data suggest that pro-inflammatory macrophages may have an impaired ability to maintain synchrony, while pro-resolution macrophages may have an enhanced ability to maintain synchrony.

Collectively, these data suggest that pro-inflammatory macrophages have weaker rhythms and impaired ability to maintain synchrony, while pro-resolution macrophages have enhanced rhythms and an increased ability to maintain synchrony. This is evidence that macrophages of different phenotypes have distinct circadian rhythms, suggesting that diversity of macrophage phenotype may lead to diversity in macrophage circadian rhythms.

Acidic pH alters circadian rhythms of macrophages.

The TME has previously been shown to be acidic, with a pH ranging from 6.8 to 6.3; much more acidic than the typical pH in blood and healthy tissue of 7.3-7.4[69-71]. There has been a previous report in which acidic pH can alter circadian rhythms, but whether this applies to macrophages remains unknown[32]. Thus, we cultured BMDMs under conditions of varying pH within a range that mimics that found within the TME (pH7.4-pH6.5). As macrophages are a heterogeneous population in the TME, we assessed the influence of acidic pH on rhythms of unstimulated, pro-resolution, and pro-inflammatory

macrophages. In line with previous observations, macrophages cultured at pH 6.5 were polarized toward a pro-resolution phenotype, characterized by increased expression of *Arg1* and *Vegf* compared to macrophages cultured at pH 7.4 (Supplementary Figure 3A). Pro-inflammatory macrophages cultured at pH 6.5 had decreased expression of *Nos2* (iNOS) compared to those cultured at pH 7.4, suggesting that an acidic pH of 6.5 both promotes a pro-resolution phenotype and suppresses a pro-inflammatory phenotype.

It has been observed that inducible cyclic AMP early repressor (*Icer*), an isoform of cyclic AMP (cAMP)-response modulator (*Crem*), is upregulated downstream of acid-sensing in macrophages, and has been used as a "biomarker" for macrophages exposed to acidic conditions in tumors. We observed induction of *Icer* in unstimulated and pro-resolution macrophages cultured at pH 6.5 compared to pH 7.4, indicating that these macrophages were sensing acidic conditions (Supplementary Figure 3B). In line with previous observations that *Icer* is induced downstream of LPS-driven TLR4 signaling, *Icer* was upregulated in pro-inflammatory macrophages compared to unstimulated macrophages even at neutral pH 7.4[72]. Although *Icer* was not further upregulated in pro-inflammatory macrophages at pH 6.5 compared to pH 7.4, *Nos2* was suppressed at pH 6.5 compared to pH 7.4, suggesting that pro-inflammatory macrophages responded to acidic pH. In all, these data confirm that macrophages of various phenotypes can sense and respond to acidic conditions within the range of pH found in the TME.

To determine whether an acidic microenvironment can influence circadian rhythms in macrophages, we assessed rhythms of unstimulated, pro-resolution, and pro-inflammatory macrophages under normal and acidic conditions. To this end, BMDMs were polarized toward a pro-resolution or a pro-inflammatory phenotype, or left unstimulated, and cultured in media at a normal pH of 7.4 or at acidic pH of 6.8 or 6.5; PER2-Luc rhythms were then observed by LumiCycle. In unstimulated and pro-resolution BMDMs, lower

204 pH led to enhanced amplitude, a shortening in period, and increased damping rate of rhythms at pH 6.8
205 and pH 6.5 relative to neutral pH 7.4 (Figure 2A,B). This suggests that in unstimulated and pro-resolution
206 macrophages, acidic pH can strengthen rhythms by enhancing amplitude and speed up the circadian
207 clock, but may impair ability to maintain synchrony. Notably, changes in amplitude and period occurred
208 in a dose-dependent fashion as pH decreased, indicating that rhythms are altered in a pH-dependent
209 manner. In contrast, pro-inflammatory macrophages cultured at pH 6.5 exhibited suppressed amplitude,
210 elongated period, and decreased damping rate of rhythms compared to those cultured at pH 7.4 (Figure
211 2C). This suggests that in pro-inflammatory macrophages, acidic pH can weaken rhythms by decreasing
212 amplitude and slow down the speed of the clock, but may promote the ability to maintain synchrony.
213 Low pH was also observed to alter the expression of the circadian clock genes *Per2*, *Cry1*, and *Nr1d1*
214 (REV-ERBα) over time across different macrophage phenotypes (Figure 2D,E,F). These data indicate that
215 exposure to acidic pH can induce changes in circadian rhythms of macrophages. Interestingly, while
216 rhythms of unstimulated and pro-resolution macrophages are enhanced under acidic pH despite
217 increased damping rate, rhythms of pro-inflammatory macrophages are suppressed under acidic
218 conditions but have improved damping rate. This suggests that acidic pH modulates rhythms differently
219 in macrophage of different phenotypes. The observation that acidic pH can enhance rhythms is
220 particularly interesting, given that acidic pH is a stressful condition that can compromise macrophage
221 survival (Supplementary Figure 4)[30].
222
223 While BMDMs are a widely used model for studying macrophages *in vitro*, there are biological
224 differences between BMDMs generated in culture and tissue-resident macrophages differentiated *in*
225 *vivo*. Thus, we sought to determine whether our observations of pH-induced changes in rhythms were
226 relevant to macrophages differentiated *in vivo*. To this end, we harvested peritoneal macrophages from
227 mice expressing PER2-Luc in the morning at ZT0 (6 AM) or in the evening at ZT12 (6 PM). Peritoneal

228 macrophages were cultured in media at neutral pH of 7.4 or acidic pH of 6.5 and observed by LumiCycle.
229 Recapitulating our results in BMDMs, peritoneal macrophages exhibited increased amplitude, decreased
230 period, and increase rate of damping at pH 6.5 compared to pH 7.4 (Figure 3A). These data indicate that
231 pH-dependent changes in circadian rhythms are relevant to *in vivo*-differentiated macrophages.
232
233 Circadian rhythms confer time-of-day variability in response to stimuli. As we have observed that acidic
234 pH can influence circadian rhythms of macrophages, we sought to understand if macrophages may be
235 more or less susceptible to pH-induced changes in rhythms depending on time of day of exposure. To
236 this end, we compared the magnitude of change in amplitude, period, and damping in peritoneal
237 macrophages when exposed to acidic pH 6.5 compared to neutral pH 7.4 at different times of day (Figure
238 3B). We observed no significant difference in the pH-driven change in amplitude, period, or damping in
239 rhythms of peritoneal macrophages taken in the morning at ZT0 compared to those taken in the evening
240 at ZT12. This indicates that the influence of pH on rhythms of macrophages was similar when exposed to
241 acidic pH in the morning or in the evening, which suggests that macrophages are similarly susceptible to
242 pH-induced changes in rhythms regardless of time of day of exposure.
243
244 **Lactate alters circadian rhythms of macrophages in a manner distinct from acidic pH.**
245
246 Elevated lactate concentrations often co-localize to regions of high acidity, due to the export of both
247 protons and lactate by glycolytic cells[73-75]. In tumors, concentration of lactate has been observed to
248 be present in concentrations of 30mM, elevated over typical lactate levels in blood and healthy tissue of
249 1.5-3mM[76]. There are previous reports that lactic acid can promote polarization of macrophages
250 toward a pro-resolution phenotype[77]. Thus, we sought to understand if lactate may be a feature of the
251 TME capable of influencing circadian rhythms of macrophages in addition to acidic pH. To this end, we

252 cultured BMDMs in the presence or absence of 25 mM sodium-L-lactate. In line with previous
253 observations, BMDMs exposed to lactate had elevated levels of *Vegf*; however, we did not observe
254 significant elevation of *Arg1* (Figure 4A)[77].
255
256 We then cultured BMDMs at normal pH 7.4 or acidic pH 6.5, in the presence or absence of 25 mM
257 sodium-L-lactate, and monitored circadian rhythms (Figure 4). Rhythms of BMDMs at pH 7.4 exposed to
258 25 mM sodium-L-lactate had elongated period and decreased damping time compared to BMDMs
259 cultured at pH 7.4 without sodium-L-lactate (Figure 4B). This suggests that lactate can slow down the
260 circadian clock and may impair the ability of macrophages to maintain synchrony. Interestingly, these
261 changes in rhythms are different from those observed in under acidic conditions, indicating that lactate
262 can modulate circadian rhythms in macrophages in a manner distinct from acidic pH.
263
264 As previously observed, macrophages exposed to acidic pH 6.5 exhibited increased amplitude, shortened
265 period, and increased damping rate of circadian rhythms. When BMDMs were exposed to both acidic pH
266 and elevated lactate, the increased amplitude observed at pH 6.5 is maintained; however, the shortened
267 period observed at pH 6.5 is lost, with period lengthened in BMDMs cultured in 25 mM sodium-l-lactate.
268 The increased damping rate of rhythms in BMDMs cultured at pH 6.5 compared to pH 7.4 is maintained,
269 and is further dampened by exposure to 25 mM sodium-l-lactate. These data indicate that changes in
270 rhythms associated with acidic conditions persisted when co-exposed to elevated lactate. In all, these
271 data indicate that concentration of lactate similar to that present in the TME can influence circadian
272 rhythms of macrophages. Lactate altered rhythms differently than acidic pH, and when macrophages
273 were exposed to acidic pH and lactate together, rhythms were further altered. This suggests that when
274 macrophages are exposed to multiple conditions capable of altering circadian rhythms, each condition
275 may contribute to a combined effect on rhythms that differs from its individual impact.

276

277 **Induction of cAMP signaling alone is not sufficient to fully drive changes in circadian rhythms**

278 **associated with acidic pH.**

279

280 Evidence in the literature suggests that acidic pH is primarily sensed by macrophages via certain G

281 protein-coupled receptors (GPCRs), inducing an increase in intracellular cAMP that drives downstream

282 signaling through the cAMP pathway[29]. Transcriptional changes downstream of cAMP signaling

283 subsequently promotes a pro-resolution phenotype[29, 78, 79]. Downstream of cAMP signaling,

284 transcription of the *Crem* isoform *Icer* is induced, which has been used as a "biomarker" for

285 macrophages exposed to acidic conditions in tumors[29]. In line with previous reports, we have

286 observed induction of *Icer* in macrophages under acidic pH, suggesting that cAMP signaling is being

287 induced under acidic conditions (Supplementary Figure 2A)[29]. This occurs as early as 2 hours,

288 concurrent with changes in rhythms, which are observed by 6 hours following exposure to acidic

289 conditions. It has been shown that induction of cAMP signaling alone is sufficient to drive a pro-

290 resolution phenotype in macrophages similar to that observed under acidic conditions[29, 78].

291 Additionally, cAMP signaling has been previously observed to modulate circadian rhythms in SCN and rat

292 fibroblasts[80, 81]. Thus, we sought to understand if the cAMP signaling pathway may be mediating the

293 pH-induced changes in circadian rhythms in macrophages.

294

295 We first sought to determine if elevation in intracellular cAMP alone was sufficient to drive changes in

296 rhythms observed in macrophages under acidic conditions. To this end, we treated macrophages with

297 forskolin, an adenylyl cyclase activator that stimulates production of cAMP, or IBMX, which drives

298 accumulation of cAMP through inhibition of phosphodiesterases (PDEs). We used a range of doses

299 similar to those previously shown to induce cAMP signaling in macrophages in the literature[29, 80, 82].

300 Treatment with either forskolin or IBMX increased amplitude of rhythms in macrophages, but not to the
301 same magnitude as acidic pH, and did not result in a changed period (Figure 5). Moreover, amplitude of
302 rhythms was not altered in forskolin- or IBMX-treated macrophages at pH 6.5, indicating neither forskolin
303 treatment nor IBMX treatment had any additional effect on rhythms under acidic conditions. These data
304 indicate that in macrophages, cAMP signaling alone induces enhanced amplitude of rhythms similar to
305 low pH, but the magnitude of this change is far less; additionally, period, which is altered under acidic
306 conditions, remains unchanged. This suggests that cAMP signaling alone may contribute to but is not
307 sufficient to fully recapitulate the changes in rhythms observed under acidic conditions.
308
309 **Adenylyl cyclase inhibitor MDL-12330A can suppress pH-mediated changes in amplitude of circadian**
310 **rhythms and pro-resolution phenotype without suppressing cAMP signaling.**
311
312 To further test whether pH-induced changes in rhythms are mediated by cAMP signaling, we treated
313 BMDMs with MDL-12330A (henceforth referred to as MDL-12), an adenylyl cyclase inhibitor which has
314 previously been shown to suppress cAMP signaling in macrophages under acidic conditions[29]. As
315 previously observed, amplitude of rhythms was enhanced in macrophages cultured at pH 6.5, while
316 period was shortened and damping rate of rhythms was increased. When BMDMs cultured at pH 6.5
317 were treated with MDL-12, the elevated amplitude of rhythms observed at pH 6.5 was suppressed
318 (Figure 6A). Notably, this occurred in a dose-dependent manner, indicating that this is a drug-dependent
319 effect. Importantly, rhythms of MDL-12-treated macrophages at pH 7.4 had similar amplitude to vehicle-
320 treated macrophages at pH 7.4. This suggests that the inhibitory effect of MDL-12 on pH-induced
321 enhancement of amplitude in macrophage rhythms was specific to signaling occurring under acidic
322 conditions. However, MDL-12 treatment of macrophages at pH 7.4 resulted in shortened period and
323 decreased damping rate compared to vehicle-treated macrophages, suggesting that MDL-12 treatment

324 had additional effects on rhythms. Despite this, MDL-12-mediated suppression of pH-driven changes in
325 amplitude, but not period or damping, suggests that the pH-driven changes in these different
326 parameters of rhythms may occur through different pathways. Interestingly, although the adenylyl
327 cyclase inhibition by MDL-12 is reported to be irreversible, we found that pretreatment up to 2 hours is
328 not sufficient to suppress pH-induced changes in amplitude. Only when macrophages continued to be
329 cultured with MDL-12 while exposed to acidic conditions was amplitude suppressed (Supplementary
330 Figure 5). Meanwhile, co-treating cells with acidic pH and MDL12 without any pre-treatment was
331 sufficient to suppress elevation of amplitude under acidic conditions (Figure 6A).
332
333 Evidence suggests that acidic pH signals through the cAMP pathway to promote a pro-resolution
334 phenotype in macrophages, with induction of *Icer* occurring directly downstream of cAMP signaling[29].
335 Despite preventing changes in amplitude under acidic pH, MDL12 treatment at the dose and treatment
336 schedule used does not suppress induction of *Icer* in macrophages under acidic conditions (Figure 6B).
337 However, induction of *Arg1* expression in macrophages under acidic conditions was suppressed by MDL-
338 12. This suggests that at the dose and treatment strategy used, MDL-12 partially suppresses the
339 response of macrophages to acidic pH by suppressing the pH-driven polarization toward a pro-resolution
340 phenotype and changes in amplitude.
341
342 To further investigate how MDL-12 was influencing cAMP signaling at the dose and treatment strategy
343 used, we evaluated phosphorylation of cyclic AMP-response element binding protein (CREB).
344 Phosphorylation of CREB occurs downstream of cAMP and has commonly been used as a readout to
345 assess induction of cAMP production in macrophages[78, 82]. In line with evidence in the literature that
346 exposure to acidic pH drives an increase in intracellular cAMP in macrophages[29], we observed that
347 downstream phosphorylation of CREB was elevated in macrophages exposed to acidic pH compared to

348 those in non-acidic conditions (Figure 6C). Unexpectedly, pCREB levels remained elevated in BMDMs at
349 pH 6.5 despite treatment with MDL-12, indicating that pH-driven phosphorylation of CREB was not
350 suppressed by MDL12 treatment. In fact, pCREB was elevated in MDL-12-treated BMDMS at pH 7.4,
351 suggesting that MDL-12 treatment alone induced phosphorylation of CREB. This is particularly surprising
352 considering that amplitude was not altered in MDL-12-treated macrophages at neutral pH 7.4 despite
353 elevated pCREB. This suggests that some elements of the cAMP signaling pathway, such as pCREB, may
354 be divorced from the pH-induced changes in rhythms. Collectively, our data indicate that while the cAMP
355 signaling pathway is induced under acidic conditions, pH-induced changes in rhythms may not be
356 attributed to cAMP signaling alone, as MDL-12 treatment suppressed pH-induced changes in amplitude
357 of rhythms, but not period or damping, without suppressing signaling through the cAMP pathway.
358
359 **There is evidence of circadian disorder in tumor-associated macrophages, which may be due to**
360 **heterogeneity in circadian rhythms within the TAM population.**
361
362 As we have observed that acidic pH at levels commonly observed in the TME can alter circadian rhythms
363 in macrophages *in vitro* and *ex vivo*, we next sought to investigate whether circadian rhythms can be
364 altered in the TME *in vivo*. Using publicly available data, we analyzed gene expression of tumor-
365 associated macrophages isolated from LLC (Lewis Lung carcinoma) tumors[83]. In line with previous
366 observations, TAMs had elevated expression of *Arg1* relative to peritoneal macrophages (Figure 7A).
367 Expression of *Crem*, which encodes *Icer*, was also elevated in TAMs, indicating that these TAMs were
368 exposed to acidic conditions within the TME (Figure 7A)[29].
369
370 To understand the status of the circadian clock in TAMs, we performed clock correlation distance (CCD)
371 analysis. This analysis has previously been used to assess functionality of the circadian clock in whole

372 tumor and in normal tissue[84]. As the circadian clock is comprised of a series of
373 transcription/translation feedback loops, gene expression is highly organized in a functional, intact clock,
374 with core clock genes existing in levels relative to each other irrespective of the time of day. In a
375 synchronized population of cells, this ordered relationship is maintained at the population level, which
376 can be visualized in a heatmap. Using previously published RNA-sequencing data of mouse peritoneal
377 macrophages[44], we found that gene co-expression of clock genes was ordered in a population of wild
378 type macrophages with functional clocks and intact circadian rhythms (Figure 7B). In contrast, clock gene
379 co-expression is disordered in BMAL1 KO macrophages with a genetic disruption of the circadian clock,
380 leading to disruption of circadian rhythms (Supplementary Figure 6). Clock correlation distance analysis
381 revealed that, similar to the BMAL1 KO peritoneal macrophages, the co-expression relationship between
382 the core circadian clock genes in TAMs is significantly more disordered than that of WT peritoneal
383 macrophages (Figure 7C). This indicates that there is population-level disorder in the circadian rhythms
384 of tumor-associated macrophages, suggesting that circadian rhythms are indeed altered in macrophages
385 within the TME.
386
387 Circadian disorder assessed by CCD has previously been used to infer disruption of circadian
388 rhythms[85]. Indeed, we observed that genetic disruption of circadian rhythms by BMAL1 KO resulted in
389 a disordered clock, as observed in peritoneal macrophages (Figure 7B). However, since CCD is a
390 population-level analysis, heterogeneity of rhythms, as observed in a desynchronous cell population,
391 rather than disruption of rhythms, may also underlie the circadian disorder observed by CCD.
392 Heterogeneity in macrophage phenotype, exposure to acidic pH, and lactate are all factors present in the
393 TME and relevant to tumor-associated macrophages. We have observed that each of these factors can
394 alter circadian rhythms in macrophages, both alone and in combination with each other. Thus, we sought

395 to understand if heterogeneity in macrophage rhythms could be contributing to the disorder in clock
396 gene co-expression and poor CCD score indicative of population-level disorder in TAM rhythms.
397
398 To address this, we examined if differences in rhythms of macrophages within a population might
399 contribute to population-level disorder as measured by CCD. To this end, we used publicly available data
400 of peritoneal macrophages taken at different times of day in four-hour intervals across two days[36]. We
401 then constructed four different sample groups in which samples were pooled according to time of day of
402 harvest. As a control population for synchronized cell population with homogenous rhythms, samples
403 taken at the same time of day were pooled. We then modeled a progressively desynchronized
404 population with increased differences in phase of rhythms by pooling samples that were taken four
405 hours apart, eight hours apart, or twelve hours apart (Figure 8A). CCD was then performed on these four
406 populations (Figure 8B). CCD score worsened as populations became increasingly desynchronized, with
407 the 12hr desynchronized population having a significantly worse CCD score than synchronized,
408 homogenous macrophage population (Figure 8C). This indicates that as circadian rhythms of individual
409 macrophages within a population become more different from each other, circadian disorder increases
410 at the population-level. This analysis suggests that heterogeneity in rhythms, as observed with
411 desynchrony, may underlie population-level disorder of the circadian clock as measured by CCD.
412 Collectively, these data suggest that rhythms are disordered in tumor-associated macrophages, and that
413 heterogeneity in macrophage rhythms within the TAM population may underlie this population-level
414 disorder in circadian rhythms of TAMs observed by CCD.
415
416 **Circadian rhythms of macrophages can influence tumor growth in a murine model of pancreatic**
417 **cancer.**
418

419 We then sought to determine how circadian rhythms in tumor-associated macrophages may influence
420 tumor growth in KCKO, which is a murine model of pancreatic ductal adenocarcinoma (PDAC)[86, 87]. To
421 this end, we used a genetic disruption of the circadian clock in macrophages. While myeloid-specific
422 genetic mouse models are useful, they are not macrophage-specific; thus, co-injection experiments are
423 commonly used to determine macrophage-specific roles[77, 88, 89]. Thus, we co-injected BMDMs from
424 WT or BMAL1 KO mice along with KCKO cells into WT mice, and tumor growth was measured. We saw a
425 significant increase in the growth of tumors co-injected with BMAL1 KO macrophages compared to those
426 co-injected with WT macrophages (Figure 9). These results suggest intact circadian rhythms of
427 macrophages can restrain tumor growth, in agreement with similar published findings in a murine model
428 of melanoma[88].
429

430 ## Discussion

431

432 Macrophages experience altered environmental conditions within the tumor microenvironment, but
433 how these may affect macrophage circadian rhythms remains unclear. Here we assessed whether
434 circadian rhythms are altered in macrophages within the TME. To this end, we explored whether
435 conditions commonly associated with the tumor microenvironment could influence circadian rhythms in
436 macrophages. As TAMs are phenotypically heterogenous, we first assessed circadian rhythms in
437 macrophages polarized toward different phenotypes. We found that polarization state affects circadian
438 rhythmicity, with pro-inflammatory macrophages exhibiting far weaker rhythms that pro-resolution
439 macrophages (Figure 1). We then modeled acidic conditions in the TME by exposing macrophages to pH
440 and lactate levels similar to those found in the TME, and found that low pH in particular dramatically
441 altered the rhythms of macrophages (Figures 2-4). Changes in cAMP signaling may contribute to these
442 changes in rhythmicity, but low pH induced alterations far beyond what is observed by enhancing cAMP

443 signaling pharmacologically (Figure 5). While the adenylyl-cyclase inhibitor MDL-12 largely rescues the
444 changes in amplitude observed in low pH, our data suggest that a pathway other than canonical cAMP
445 signaling may be involved in this effect (Figure 6). Finally, we assessed the status of the circadian clock in
446 tumor-associated macrophages, the potential contribution of heterogeneity in circadian rhythms to
447 population-level rhythms, and assessed whether the circadian regulation of macrophages impacts tumor
448 growth. Our results indicate that macrophage rhythms as a whole are disordered within tumors (Figure
449 7), and that heterogeneity in rhythms within the tumor-associated macrophage population may underlie
450 this observed circadian disorder (Figure 8). We further demonstrated that the intact macrophage
451 circadian clock can suppress tumor growth (Figure 9). Overall, our results for the first time demonstrate
452 that exposure of macrophages to conditions associated with the tumor microenvironment can influence
453 circadian rhythms, a key aspect of macrophage biology.
454
455 A critical question in understanding the role of circadian rhythms in macrophage biology is determining
456 how different polarization states of macrophages affect their internal circadian rhythms. This is
457 especially important considering that tumor-associated macrophages are a highly heterogeneous
458 population. Our data indicate that compared to unstimulated macrophages, rhythms are enhanced in
459 pro-resolution macrophages, characterized by increased amplitude and improved ability to maintain
460 synchrony; in contrast, rhythms are suppressed in pro-inflammatory macrophages, characterized by
461 decreased amplitude and impaired ability to maintain synchrony (Figure 1). These agree with the
462 findings of others which have shown that polarizing stimuli alone and in combination with each other
463 can alter rhythms differently in macrophages[64, 65]. In a tumor, macrophages exist along a continuum
464 of polarization states and phenotypes[18-21, 24]. Thus, while our characterizations of rhythms in *in vitro*-
465 polarized macrophages provide a foundation for understanding how phenotype affects circadian
466 rhythms of macrophages, further experiments will be needed to assess macrophages across the full

467 spectrum of phenotypes. Indeed, alteration of rhythms may be just as highly variable and context-
468 dependent as phenotype itself.
469
470 In addition to polarizing stimuli, tumor-associated macrophages are exposed to a variety of conditions
471 within the tumor microenvironment that may alter their circadian rhythms. We observed that exposure
472 to acidic pH alters rhythms in macrophages, increasing amplitude of pro-resolution macrophages but
473 suppressing amplitude of pro-inflammatory macrophages (Figure 2). This indicates that pH affects
474 rhythms differently depending on phenotype, hinting at additional layers of complexity in how the
475 environment could contribute to changes in circadian rhythms. Even further changes in rhythms were
476 observed when macrophages were exposed to lactate in conjunction with acidic pH (Figure 4). These
477 observations suggest that the combination of stimuli present in the microenvironment such as lactate
478 and low pH, as well as various polarizing stimuli, can each contribute to modulate rhythms, resulting in
479 highly context-dependent changes in circadian rhythms of macrophages based on the
480 microenvironment. As macrophages are highly plastic and are exquisitely capable of sensing and
481 responding to their environment, one could reason that changes in circadian rhythms, and downstream
482 circadian regulation, are a mechanism by which macrophages can adopt different programs to respond
483 to their environment.
484
485 It was previously observed that acidic pH can disrupt circadian rhythms in cell lines[32]. However, while
486 acidic pH alters rhythms in macrophages, it does not ablate them. This suggests that the influence of
487 acidic pH on circadian rhythms can vary between cell types. pH-induced circadian disruption was found
488 to be driven by inhibition of mTORC1 activity in cell lines, and there was evidence to suggest that
489 mTORC1 activity was sensitive to pH in T cells [90]. Thus, the role of mTORC1 activity in mediating pH-
490 driven changes in circadian rhythms of macrophages will be a topic of future investigation.

491

492 The mechanism through which acidic pH can modulate the circadian clock in macrophages remains
493 unclear. Evidence in the literature suggests that acidic pH promotes a pro-resolution phenotype in
494 macrophages by driving signaling through the cAMP pathway[29]. It has previously been shown that
495 cAMP signaling can modulate the circadian clock[81]. However, our data indicate that cAMP signaling is
496 not fully sufficient to confer pH-mediated changes in circadian rhythms in macrophages. Treatment with
497 forskolin or IBMX enhanced amplitude of oscillation, but was not sufficient to fully recapitulate pH-
498 induced changes in rhythms (Figure 5). Interestingly, treatment with MDL-12, commonly known as an
499 inhibitor of adenylyl cyclase[29, 91], resulted in suppression of pH-induced changes in amplitude of
500 circadian rhythms and alleviated pH-mediated polarization toward a pro-resolution phenotype,
501 measured by *Arg1* expression (Figure 6). However, our data indicate that treatment with MDL-12 at the
502 dose and treatment strategy used did not inhibit signaling through the cAMP signaling pathway, as *Icer*
503 induction and phosphorylation of CREB were not suppressed. While MDL-12 is commonly used as an
504 adenylyl cyclase inhibitor, it has also been documented to have inhibitory activity toward
505 phosphodiesterases (PDEs) and the import of calcium into the cytosol through various mechanisms[92,
506 93]. This is of particular interest, as calcium signaling has also been shown to be capable of modulating
507 the circadian clock[94]. Furthermore, while acid-sensing through GPCRs have been the most well-
508 characterized pathways in macrophages, there remain additional ways in which acidic pH can be sensed
509 by macrophages such as acid-sensing ion channels[95, 96]. Further work is required to understand the
510 signaling pathways through which pH can influence macrophage phenotype and circadian rhythms.

511

512 Taken together, our findings indicate that both macrophage polarization state and exposure to
513 environmental conditions such as low pH and lactate each affect the circadian rhythms of macrophages.
514 One prominent question that remains elusive is whether circadian rhythms of macrophages are

515 governed by phenotype, or whether phenotype is subject to control of circadian rhythms. Alternately,
516 the relationship between the two could very well be bi-directional. Acidic pH promotes a pro-resolution
517 phenotype and suppresses pro-inflammatory activity as early as 2 hours post-exposure (Supplementary
518 Figure 3), with changes in rhythms observed by 12 hours (Figure 2). This suggests that pH-driven changes
519 in phenotype may precede changes in rhythms. How much the pH-driven changes in rhythms is
520 influenced directly by pH sensing, or indirectly through the influence of pH on phenotype, remains
521 unknown. Certainly, polarization toward a pro-resolution phenotype and exposure to acidic pH each
522 have different effects on circadian rhythms of macrophages; while polarization of macrophages toward a
523 pro-resolution phenotype increases amplitude and decreases damping rate of circadian rhythms,
524 exposure to acidic pH not only increases amplitude, but shortens period and increases damping rate of
525 rhythms (Figures 1, 2). Additionally, acidic pH drives changes in rhythms of pro-resolution macrophages
526 similar to that of unstimulated macrophages, suggesting that the signaling driving these changes in
527 rhythms are not redundant between the two conditions. This suggests that acidic pH-promoted
528 polarization toward a pro-resolution phenotype does not on its own account for the pH-driven changes
529 in rhythms. Studies have shown that circadian rhythms are regulated by metabolism[97], and it is well-
530 appreciated that macrophages of distinct phenotypes prioritize different metabolic pathways[98]. Thus,
531 the metabolic needs of macrophages of different phenotypes likely influences the response to pH and
532 other metabolically stressful conditions in the TME, and downstream effects on circadian rhythms.
533 Indeed, we observed that exposure to acidic pH had an opposite effect on rhythms of pro-inflammatory
534 macrophages compared to pro-resolution macrophages (Figure 2). Further work is required to
535 understand the interplay between macrophage phenotype, metabolism, and circadian rhythms.
536
537 We observed that acidic pH appears to enhance circadian rhythms of unstimulated and pro-resolution
538 macrophages, and we and others have shown evidence that macrophages are exposed to an acidic

539 environment within the TME[28, 29]. However, analysis of TAMs by clock correlation distance (CCD)
540 presents evidence that rhythms are disordered in TAMs (Figure 7). CCD is one of the most practical tools
541 currently available to assess circadian rhythms due to its ability to assess rhythms independent of time
542 of day and without the need for a circadian time series, which is often not available in publicly available
543 data from mice and humans[84]. However, CCD has some limitations, primary of which is that it is a
544 measure of population-level circadian rhythms. There is currently a major barrier in the circadian field in
545 the ability to measure circadian rhythms at the single-cell level. Some recent work has defined single-
546 cell rhythms and uncovered a surprising amount of heterogeneity in mouse and fly tissues[99-101]**.** A full
547 measure of single-cell circadian dynamics within a tissue must be assessed to facilitate studies of
548 rhythms *in vivo* where cell populations are highly heterogeneous, such as within the tumor
549 microenvironment or at a site of infection. Indeed, we present evidence that heterogeneity of circadian
550 rhythms within a given population may underlie this observed circadian disorder (Figure 8). We have
551 shown that various stimuli can alter rhythms of macrophages in a complex and contributing manner,
552 including polarizing stimuli, acidic pH, and lactate. TGFβ is produced by a variety of cells within the TME,
553 and was recently identified as a signal that can modulate circadian rhythms[102, 103]. Thus, it is
554 conceivable that, in addition to acidic pH, other stimuli in the TME are influencing circadian rhythms to
555 drive population-level disorder that we are observing by CCD. Notably, we cannot rule out that the
556 disorder observed by CCD may be indicative of circadian disruption.
557
558 In light of our observations that conditions associated with the TME can alter circadian rhythms in
559 macrophages, it becomes increasingly important to understand the relevance of macrophage rhythms to
560 their function in tumors. Data from our lab and others suggest that disruption of the macrophage-
561 intrinsic circadian clock accelerates tumor growth, indicating that circadian regulation of macrophages is
562 tumor-suppressive[88]. This agrees with complementary findings that behavioral disruption of circadian

563 rhythms in mice (through chronic jetlag) disrupts tumor macrophage circadian rhythms and accelerates
564 tumor growth[56]**.** It remains unclear whether this is through the pro-tumorigenic functions of
565 macrophages such as extracellular matrix remodeling or angiogenesis, through suppression of the anti-
566 tumor immune response, or a combination of both functions. Further work will be needed to tease apart
567 these distinctions.
568
569 Whereas much work has been done to characterize how macrophages are regulated within the TME, the
570 impact of the TME on circadian rhythms of macrophages remained elusive. Our work uncovers a novel
571 way in which conditions associated with the TME can influence macrophage biology through modulation
572 of circadian rhythms. While the majority of studies investigating the circadian regulation of macrophages
573 have been conducted studying macrophages under homeostatic conditions or in response to acute
574 inflammation[36, 38, 44, 45, 104], our work contributes to an emerging body of evidence that the tissue
575 microenvironment can influence circadian rhythms[102]. This is increasingly important when considering
576 the role of circadian rhythms in immune responses at sites of ongoing, chronic inflammation where the
577 microenvironment is altered, such as within tumors. In identifying factors within the TME that can
578 modulate circadian rhythms of macrophages and uncovering evidence of circadian disorder within
579 tumor-associated macrophages, this work lays the foundation for further studies aimed at understanding
580 how the TME can influence the function of tumor-associated macrophages through modulation of
581 circadian rhythms.
582
583 **Limitations of the Study**
584
585 Our observations of rhythms in macrophages of different phenotypes are limited by *in vitro* polarization
586 models. It is important to note that while our data suggest that pro-inflammatory macrophages have

587 suppressed rhythms and increased rate of desynchrony, it remains unclear the extent to which these
588 findings apply to the range of pro-inflammatory macrophages found *in vivo*. We use IFNγ and LPS co-
589 treatment *in vitro* to model a pro-inflammatory macrophage phenotype that is commonly referred to as
590 'M1', but under inflammatory conditions *in vivo*, macrophages are exposed to a variety of stimuli that
591 result in a spectrum of phenotypes, each highly context-dependent. The same is true for for 'M2';
592 different tissue microenvironment are different and pro-resolution macrophages exist in a spectrum.
593 Rhythms were heavily suppressed in pro-inflammatory macrophages, which makes analysis of rhythm
594 parameters in pro-inflammatory macrophages more challenging as amplitude and signal reaches limit of
595 detection. We assessed parameters of oscillation using LumiCycle Analysis, a method commonly used in
596 the circadian field[64, 105]. Our observations of changes in amplitude and period in pro-inflammatory
597 macrophages compared to unstimulated macrophages agrees with the literature, where these changes
598 in rhythms have been observed using LumiCycle as well as by mRNA[64, 65]. This supports the validity
599 and reproducibility of our observations despite the challenges of observing and analyzing rhythms of
600 pro-inflammatory macrophages.
601

602 Methods

603 **Animals**

604 Mice were maintained in individually ventilated cages with bedding and nesting material in a
605 temperature-controlled, pathogen-free environment in the animal care facility at the University of
606 Rochester. All animal protocols were approved by the University of Rochester Committee of Animal
607 Resources (UCAR). All experiments were performed in compliance with the NIH- and University of
608 Rochester-approved guidelines for the use and care of animals, as well as recommendations in the Guide
609 for the Care and Use of Laboratory Animals of the National Research Council[106]. Mice were housed on
610 a 12:12 light dark cycle. In some cases, to ease timepoint collection, mice were housed under reverse

611 lighting conditions in a 12:12 dark light cycle for at least 2 weeks prior to use in experiments. Mice used
612 for experiments were between the ages of 8-14 weeks old; both male and female mice were used. Mice
613 were euthanized humanely prior to harvesting peritoneal macrophages or bone marrow.
614
615 Previously characterized mice with a myeloid-specific deletion of BMAL1 (LysM-cre$^{+/-}$Bmal1$^{flox/flox}$;
616 referred to as BMAL1 KO mice)[45] in a C57BL/6 background were generated by crossing LysM-cre
617 mice[107] with Bmal1$^{flox/flox}$ mice[108]. These mice were further crossed with PER2-Luc mice[61] to
618 generate BMAL1 KO or wild-type control mice (LysM-cre$^{-/-}$Bmal1$^{flox/flox}$; referred to as WT) expressing
619 PER2-Luc. PER2-Luc (strain #006852), LysM-cre (strain #004781), and Bmal1$^{flox/flox}$(strain #007668) mice
620 used for breeding to generate WT and BMAL1 KO mice were purchased from the Jackson Laboratory.
621
622 **Differentiation and culture of bone marrow-derived macrophages**
623 Bone marrow-derived macrophages (BMDMs) were generated from bone marrow isolated from WT
624 mice using a well-established protocol for differentiation of BMDMs over 7 days[109, 110]. In brief, bone
625 marrow cells were seeded at 200,000 cells/mL on non-tissue culture treated-plates in BMDM
626 Differentiation Media: RPMI (Corning, CAT#MT10040CV) supplemented with 20% (v/v) L929 supernatant
627 and 10% (v/v) heat-inactivated (HI) fetal bovine serum (FBS) (Cytiva, CAT#SH30396.03), supplemented
628 with 100 U/mL Penicillin-Streptomycin (Gibco, CAT# 15140122). Cells were grown at 37°C in air enriched
629 with 5% CO_2. On day 3, additional BMDM Differentiation Media was added to cells. On day 6 of the
630 differentiation protocol, BMDMs were seeded at $1.2*10^6$ cells/mL and left in BMDM Differentiation
631 Media, and kept at 37°C in air enriched with 5% CO_2. On day 7, BMDM Differentiation Media was
632 removed and BMDMs were synchronized.
633

634 To synchronize BMDMs, BMDMs were first serum starved for 24 hours in serum-free media (RPMI,
635 supplemented with 100 U/mL Penicillin-Streptomycin); BMDMs were then subjected to serum shock by
636 replacing serum-free media with RPMI supplemented with 50% (v/V) HI horse serum (Corning,
637 CAT#35030CV) at 37°C in air enriched with 5% CO_2. At the end of this synchronization protocol, media
638 was replaced with Atmospheric Media, which has been formulated for use at atmospheric CO_2 levels and
639 enhanced pH stability by increasing buffering capacity at low pH[32]: RPMI (Corning, CAT#50-020-PC),
640 25mM HEPES (Gibco, CAT#15630080), 25mM PIPES (Sigma, CAT#P1851), supplemented with 10% (v/v)
641 HI FBS and 100 U/mL Penicillin-Streptomycin. Atmospheric Media was adjusted to pH 7.4, 6.8, or 6.5
642 with NaOH and filter-sterilized.
643
644 BMDMs cultured in Atmospheric Media at pH 7.4, 6.8, or 6.5 were either left unstimulated or were
645 polarized toward a pro-resolution ('M2') or pro-inflammatory phenotype ('M1') by addition of 10 ng/mL
646 IL-4 (PeproTech, CAT#214-14) and 10 ng/mL IL-13 (PeproTech, CAT# 210-13), or 50 ng/mL IFNγ
647 (PeproTech, CAT#315-05) and 100 ng/mL LPS (Invitrogen, CAT#00497693), respectively. For lactate
648 experiments, sodium-L-lactate (Sigma, CAT#L7022) or vehicle was added to Atmospheric Media for 25
649 mM sodium-L-lactate or 0 mM sodium-L-lactate in Atmospheric Media. For interrogation of cAMP
650 signaling pathway, BMDMs were cultured in Atmospheric Media at pH 7.4 or 6.5 with vehicle or 5, 10, or
651 15 µM MDL-12330A (Sigma, CAT#M182). For phenocopy experiments (Figure 5), BMDMs were not
652 synchronized prior to the experiment. BMDMs were cultured in Atmospheric Media at pH 7.4 or 6.5 with
653 vehicle or 20, 40, or 80 µM IBMX (Sigma, CAT#I5879) or forskolin (Sigma, CAT#344270). For LumiCycle
654 experiments, 100mM D-luciferin was added to Atmospheric Media at 1:1000 for 100µM D-luciferin
655 (Promega, CAT#E1602). Cells cultured in Atmospheric Media were kept at 37°C in atmospheric
656 conditions, and were either monitored over time by LumiCycle or harvested for RNA or protein at the
657 time points indicated.

658

659 **Isolation and culture of peritoneal macrophages**

660 Peritoneal exudate cells were harvested from mice as previously published[111]. To isolate peritoneal
661 macrophages, peritoneal exudate cells were seeded at $1.2*10^6$ cells/mL in RPMI/10% HI FBS
662 supplemented with 100U/mL Penicillin-Streptomycin and left at 37°C for 1 hour, after which non-
663 adherent cells were rinsed off[110]. Peritoneal macrophages were then cultured in Atmospheric Media
664 at pH 7.4 or 6.5 with 100µM D-luciferin, and kept at 37°C in atmospheric conditions.

665

666 **Quantification of circadian rhythm parameters**

667 Using the Lumicycle Analysis program version 2.701 (Actimetrics), raw data was fitted to a linear
668 baseline, and the baseline-subtracted data was fitted to a damped sin wave from which period and
669 damping were calculated[105]. Amplitude was calculated from baseline-subtracted data by subtracting
670 the bioluminescent values of the first peak from the first trough as previously published[64].

671

672 **Quantitative PCR**

673 Cells were lysed and RNA was isolated using the E.Z.N.A. HP Total RNA Kit (Omega BioTek, CAT#R6812-
674 02). RNA was reverse transcribed to cDNA using the ABI Reverse Transcription Reagents system, using
675 oligo dT for priming (Applied Biosystems, CAT#N8080234). qPCR was performed with cDNA using
676 PerfeCTa SYBR Green FastMix (QuantaBio, CAT#95074-05K) and with the Quant Studio 5 quantitative PCR
677 machines (Applied Biosystems). Triplicate technical replicates were performed, outlier replicates (defined
678 as being more than 1 Ct away from other two replicates) were discarded, and relative mRNA was
679 normalized to *Tbp* and assessed by the ΔΔCt. The following primers were used: *Tbp* (5'-
680 CCAGAACTGAAAATCAACGCAG-3', 5'-TGTATCTACCGTGAATCTTGGC-3') (IDT, Mm.PT.39a.22214839), *Arg1*
681 (5'-CTCCAAGCCAAAGTCCTTAGAG-3', 5'-AGGAGCTGTCATTAGGGACATC-3')[112], *Vegf* (5'-

682 CCACGACAGAAGGAGAGCAGAAGTCC-3', 5'-CGTTACAGCAGCCTGCACAGCG-3')[77], *Nos2* (5'-
683 GCTTCTGGTCGATGTCATGAG-3', 5'-TCCACCAGGAGATGTTGAAC-3'), *Icer* (5'-ATGGCTGTAACTGGAGATGAA-
684 3', 5'-GTGGCAAAGCAGTAGTAGGA-3')[29], *Per2* (5'-TGAGGTAGATAGCCCAGGAG-3,' 5'-
685 GCTATGAAGCGCCTAGAATCC-3') (IDT, Mm.PT.58.5594166), *Cry1* (5'-GCTATGCTCCTGGAGAGAACG T-3,' 5'-
686 TGTCCCCGTGAGCATAGTGTAA-3')[113], *Nr1d1* (5'-GAGCCACTAGAGCCAATGTAG-3,' 5'-
687 CCAGTTTGAATGACCGCTTTC-3') (IDT, Mm.PT.58.17472803).
688
689 **Western blot**
690 Cells were lysed using the M-Per lysis reagent (Thermo Scientific, CAT#78501), supplemented with
691 protease and phosphatase inhibitor cocktail (1:100; Sigma, CAT#PPC1010) and phosphatase inhibitor
692 cocktail 2 (1:50; Sigma, CAT#P5726), with 200µM deferoxamine (Sigma, CAT#D9533). Lysates were
693 incubated on ice for 1 hour, then centrifuged at 17,000 xg to pellet out debris; supernatant was
694 collected. Protein was quantified using the Bio-Rad DC Protein Assay Kit (Bio-Rad, CAT#5000112), and
695 lysates of equal concentration were prepared and run by SDS-PAGE on Bio-Rad Criterion 4–15% 26-well
696 gradient gel (Bio-Rad, CAT#5678095). Gels were transferred using the Trans-Blot Turbo system (Bio-Rad)
697 to nitrocellulose membranes (Bio-Rad CAT#1704271).
698
699 The following primary antibody was used: rabbit anti-p-CREB (Ser133, Ser129) (Invitrogen, CAT#44-
700 297G). The following secondary antibody was used: goat anti-rabbit Alexa Fluor 680 (Invitrogen,
701 CAT#A21109). Of note, two different anti-CREB antibodies were tested (Cell Signaling, CAT#9197 and
702 Invitrogen, CAT#35-0900) in combination with the appropriate secondary antibody, but neither revealed
703 bands at the correct molecular weight for CREB protein. Membranes were digitally imaged using a
704 ChemiDoc MP (Bio-Rad) and uniformly contrasted. Total protein was imaged by Stain-Free imaging

705 technology (Bio-Rad) and used as loading control. To visualize total protein, image of entire membrane
706 was shrunk to match the size of pCREB.
707
708 **Survival under acidic pH**
709 BMDMs were seeded, in triplicate, at $1.2*10^6$ cells/mL in a 96-well plate. BMDMs were synchronized,
710 then cultured in Atmospheric Media at pH 7.4, 6.8, or 6.5 containing 10 ng/mL IL-4 and 10 ng/mL IL-13,
711 or 50 ng/mL IFNγ and 100 ng/mL LPS, or vehicle for unstimulated control. BMDMs were fixed at 1, 2, and
712 3 days later. BMDMs were stained with DAPI, and plates were imaged using a Celigo S. Number of nuclei
713 per well was enumerated using Celigo software to quantify the number of adherent BMDMs after time in
714 culture under acidic conditions as a readout of survival.
715
716 **Tumor growth**
717 Mice were anesthetized via inhalation of 4 vol% isoflurane in 100% oxygen at a flow rate of 4 L/min prior
718 to injection. Following application of 70% ethanol to the site of injection, with $1*10^6$ WT or BMAL1 KO
719 macrophages and $1*10^6$ KCKO cells in 100 uL saline were subcutaneously co-injected in the flank of WT
720 mice. In line with previously published co-injection tumor experiments, mice were injected with
721 macrophages at a 1:1 ratio[77, 88]. Tumor growth was measured by caliper, and volume was calculated
722 by the modified ellipsoidal formula: tumor volume = $0.5*(\text{length}*\text{width}^2)$[114]. Mice were euthanized
723 when there was ulcer formation or when tumor size reached a diameter of 20mm.
724
725 **Processing and analysis of publicly available gene expression data**
726 FASTQ files from a previously published analysis of peritoneal macrophages from WT or BMAL1 KO mice
727 were downloaded from EMBL- European Bioinformatics Institute Array Express (accession #E-MTAB-
728 8411)[44]. For these samples, multiple files of the same run were concatenated before mapping. FASTQ

729 files from a previous published study of tumor-associated macrophages were downloaded from NCBI
730 GEO (accession #GSE188549)[83]. Both sets of samples were mapped to transcripts using Salmon 1.3.0
731 in mapping-based mode using a decoy-aware transcription built from the Gencode M25 GRCm38
732 primary assembly mouse genome and M25 mouse transcriptome[115]. Single-end mapping was used
733 for GSE188549 samples and paired-end mapping was used for E-MTAB-8411. All transcripts were then
734 collapsed to gene-level using Tximport v1.14.2with the Gencode M25 transcriptome, and genes were
735 annotated with symbols using the Ensembl GRCm38.100 transcriptome annotations[116]. Transcripts
736 per million (TPM) outputted from Tximport were used for downstream analyses. CEL files from a
737 previously published time series analysis of peritoneal macrophages from WT mice were downloaded
738 from NCBI GEO (accession #GSE25585)[36]. Microarray data was imported and analyzed from CEL files
739 using the packages affy and Limma, and genes were annotated with symbols using the University of
740 Michigan Brain Array Custom CDF v25.0 for the Mouse Gene 1.0 ST Array[117, 118]. Clock correlation
741 distance analysis was performed as previously described[84].
742
743 **Data sharing**
744 Raw data will be provided by uploading to FigShare, as will R code used for data analysis.
745

746 Acknowledgements

747 We would like to thank Dr. Jim Miller (Department of Microbiology and Immunology, University of
748 Rochester, NY) and Dr. Paul Brookes (Department of Anesthesiology and Perioperative Medicine,
749 University of Rochester, NY) for their intellectual contributions. All visual illustrations were made using
750 BioRender. The project described was supported by Award Number T32AI007285 (to AMKC) from the
751 National Institute of Allergy and Infectious Diseases, Grant Number T32 GM135134 (to AMKC) from the
752 National Institutes of Health, Grant Number R00CA204593 (to BJA) from the National Cancer Institute of

753 the National Institutes of Health, and the Wilmot Predoctoral Cancer Research Fellowship (to AMKC)
754 from the Wilmot Cancer Institute.
755

756 Author Contributions

757 Conceptualization: Amelia M. Knudsen-Clark, Brian J. Altman
758 Data Curation: Amelia M. Knudsen-Clark, Brian J. Altman
759 Formal analysis: Amelia M. Knudsen-Clark, Brian J. Altman, Lauren M. Hablitz
760 Funding acquisition: Brian J. Altman, Amelia M. Knudsen-Clark
761 Investigation: Amelia M. Knudsen-Clark, Juliana Cazarin, Daniel Mwangi
762 Methodology: Amelia M. Knudsen-Clark, Brian J. Altman, Minsoo Kim
763 Resources: Brian J. Altman
764 Software: Brian J. Altman, Amelia M. Knudsen-Clark, Daniel Mwangi
765 Supervision: Brian J. Altman
766 Validation: Amelia M. Knudsen-Clark
767 Writing – original draft: Amelia M. Knudsen-Clark
768 Writing – review and editing: Amelia M. Knudsen-Clark, Juliana Cazarin, Brian J. Altman, Daniel Mwangi,
769 Minsoo Kim, Lauren M. Hablitz.
770

771 Conflict of Interest

772 The authors declare no conflict of interest.
773

774 Figure Legends

775 **Figure 1. Macrophages of different phenotypes have distinct circadian rhythms.** Bone marrow-derived
776 macrophages (BMDMs) were obtained from C57BL/6 mice expressing PER2-Luc. The circadian clocks of
777 BMDMs were synchronized by a 24-hour period of serum starvation in media with 0% serum, followed
778 by a 2-hour period of serum shock in media with 50% serum. Luciferase activity of BMDMs stimulated
779 with either 10 ng/mL IL-4 and 10 ng/mL IL-13, or 50 ng/mL IFNγ and 100 ng/mL LPS; or left unstimulated
780 was monitored in real time by LumiCycle. Data was baseline-subtracted using the running average.
781 Oscillation parameters of BMDMs were measured by LumiCycle Analysis. Shown are mean and standard
782 error of the mean (SEM), n=5 biological replicates. Statistical significance determined by unpaired two-
783 tailed T test with Welch's correction; *, $p < 0.05$; **, $p<0.005$; ***, $p<0.0005$. Data shown are
784 representative of 2 independent experiments.
785
786 **Figure 2. Acidic pH alters circadian rhythms of bone marrow-derived macrophages *in vitro*.** Bone
787 marrow-derived macrophages (BMDMs) were obtained from C57BL/6 mice expressing PER2-Luc. The
788 circadian clocks of BMDMs were synchronized by a 24-hour period of serum starvation in media with 0%
789 serum, followed by a 2-hour period of serum shock in media with 50% serum. BMDMs were then
790 cultured in media with neutral pH 7.4 or acidic media with pH 6.8 or 6.5, and stimulated with either 10
791 ng/mL IL-4 and 10 ng/mL IL-13 (B, E), or 50 ng/mL IFNγ and 100 ng/mL LPS (C, F); or left unstimulated (A,
792 D). Luciferase activity was monitored in real time by LumiCycle (A, B, C). Shown are mean and SEM, n=2
793 biological replicates, representative of 2 independent experiments. Data from both experiments was
794 baseline-subtracted using the running average, and oscillation parameters were measured by LumiCycle
795 Analysis. Shown are mean and SEM, n=5 biological replicates. In parallel, RNA was collected at 12, 16, 20,
796 and 24 hours post-synchronization, and qt-PCR was performed to assess oscillation of transcripts
797 encoding core clock proteins in macrophages under acidic conditions (D, E, F). Shown are mean and SEM,
798 n=3 biological replicates. Data shown are representative of 2 independent experiments. Statistical

799 significance determined by unpaired two-tailed T test with Welch's correction; *, $p < 0.05$; **, $p<0.005$;
800 ***, $p<0.0005$.
801
802 **Figure 3. Acidic pH alters circadian rhythms of bone marrow-derived macrophages *ex vivo* at**
803 **temporally distinct times of day.** Peritoneal macrophages were obtained at ZT0 or ZT12 from C57BL/6
804 mice expressing PER2-Luc and cultured in media with neutral pH 7.4 or acidic pH 6.5. Luciferase activity
805 was monitored in real time by LumiCycle (A). Shown are mean and SEM, n=2 biological replicates,
806 representative of 2 independent experiments. Data from both experiments was baseline-subtracted
807 using the running average, and oscillation parameters were measured by LumiCycle Analysis; shown are
808 mean and SEM, n=4 biological replicates. Statistical significance determined by unpaired two-tailed T test
809 with Welch's correction. The magnitude of change in circadian oscillation parameters between
810 macrophages at pH 7.4 and pH 6.5 was compared between peritoneal macrophages taken at ZT 0 or ZT
811 12 (B). Shown is the mean and SEM, n=4; data pooled from the 2 independent experiments in (A).
812 Statistical significance determined by paired two-tailed T test with Welch's correction; *, $p < 0.05$; **,
813 $p<0.005$; ***, $p<0.0005$.
814
815 **Figure 4. Lactate alters circadian rhythms in macrophages, both alone and in conjunction with acidic**
816 **pH.** Bone marrow-derived macrophages (BMDMs) were obtained from C57BL/6 mice expressing PER2-
817 Luc. The circadian clocks of BMDMs were synchronized by a 24-hour period of serum starvation in media
818 with 0% serum, followed by a 2-hour period of serum shock in media with 50% serum. BMDMs were
819 then cultured in media with neutral pH 7.4 or acidic pH 6.5, supplemented with 0 mM or 25 mM sodium-
820 L-lactate. RNA was collected at 6 hours post-treatment, and expression of pro-resolution phenotype
821 markers *Arg1* or *Vegf* was quantified by qtPCR (A). Shown is the mean and SEM, n=6 biological replicates,
822 data pooled from 2 independent experiments. Luciferase activity was monitored in real time by

823 LumiCycle (B). Shown is the mean and SEM, n=4 biological replicates; data representative of 2
824 independent experiments. Data from both experiments was baseline-subtracted using the running
825 average, and oscillation parameters were measured by LumiCycle Analysis. Shown is the mean and SEM,
826 n=7-10 biological replicates. Statistical significance determined by unpaired two-tailed T test with
827 Welch's correction; *, $p < 0.05$; **, $p<0.005$; ***, $p<0.0005$; ****, $p<0.00005$.
828
829 **Figure 5. Treatment with Forskolin or IBMX does not fully recapitulate pH-driven changes in circadian**
830 **rhythms of macrophages.** Bone marrow-derived macrophages (BMDMs) were obtained from C57BL/6
831 mice expressing PER2-Luc. BMDMs were cultured in media with neutral pH 7.4 or acidic pH 6.5, and
832 treated with vehicle or 20, 40 or 80 uM Forsokolin (A), or treated with vehicle or 20, 40, 80 uM IBMX (B).
833 Luciferase activity was monitored in real time by LumiCycle. Data was baseline-subtracted using the
834 running average. Shown is the mean, n=2 biological replicates. Data shown are representative of 2
835 independent experiments.
836
837 **Figure 6. Treatment with MDL-12 suppresses pH-induced changes in amplitude of circadian rhythms**
838 **without suppressing signaling through the cAMP signaling pathway under acidic conditions.** Bone
839 marrow-derived macrophages (BMDMs) were obtained from C57BL/6 mice expressing PER2-Luc. The
840 circadian clocks of BMDMs were synchronized by a 24-hour period of serum starvation in media with 0%
841 serum, followed by a 2-hour period of serum shock in media with 50% serum. BMDMs were then
842 cultured in media with neutral pH 7.4 or acidic pH 6.5, and treated with vehicle or 5, 10, or 15uM MDL-
843 12. Luciferase activity was monitored in real time by LumiCycle. Data was baseline-subtracted using the
844 running average, and oscillation parameters were measured by LumiCycle Analysis (A). Shown is the
845 mean, n=4 biological replicates. Expression of genes associated with acid sensing (*Icer*) and pro-
846 resolution phenotype (*Arg1*) was measured (B). Shown is the mean and SEM; n=3 biological replicates.

847 Phosphorylation of CREB was assessed (C). Statistical significance determined by unpaired two-tailed T
848 test with Welch's correction; *, $p < 0.05$; **, $p<0.005$; ***, $p<0.0005$; ****, $p<0.00005$. Data shown are
849 representative of 2-3 independent experiments.
850
851 **Figure 7. Clock correlation distance (CCD) analysis provides evidence of circadian disorder in tumor-**
852 **associated macrophages.** RNAseq datasets of WT peritoneal macrophages (n=5), BMAL1 KO peritoneal
853 macrophages (n=4), and tumor-associated macrophages (TAMs, n=10) were analyzed for expression of
854 *Arg1* and *Crem* (A). Statistical significance determined by one-way ANOVA with Turkey's multiple
855 comparison test; ****, $p<0.00005$. Clock correlation distance (CCD) analysis was performed (B) and
856 statistical analysis to compare CCD scores was performed by calculating delta CCD; *, $p<0.05$ (C).
857
858 **Figure 8. Heterogeneity in circadian rhythms of cells within a population can lead to circadian disorder**
859 **observed by CCD.** Increasingly desynchronized populations were modeled using an RNAseq data set of
860 WT peritoneal macrophages (n=12) taken at 4-hour intervals across two days. A schematic of the
861 populations used in experimental design (A). Clock correlation distance (CCD) analysis was performed (B)
862 and statistical analysis to compare CCD scores was performed by calculating delta CCD (C).
863
864 **Figure 9. A functional circadian clock in macrophages can influence tumor growth in a murine model of**
865 **PDAC.** Bone marrow-derived macrophages (BMDMs) obtained from WT or BMAL1 KO mice were
866 subcutaneously co-injected with KCKO cells into the flank of WT mice. Tumor growth was measured by
867 caliper. Shown is the mean and SEM; n=20 individual mice, 10 male and 10 female. Statistical significance
868 determined at each time point by unpaired two-tailed T test with Welch's correction; *, $p < 0.05$; **,
869 $p<0.005$; ***, $p<0.0005$. Data shown are representative of 2 independent experiments.
870

871 **Supplemental Figure 1. Polarization of macrophages toward pro-resolution or pro-inflammatory**
872 **phenotype.** Bone marrow-derived macrophages (BMDMs) were derived from C57BL/6 mice expressing
873 PER2-Luc. The circadian clocks of BMDMs were synchronized by a 24-hour period of serum starvation in
874 media with 0% serum, followed by a 2-hour period of serum shock in media with 50% serum. BMDMs
875 were then stimulated with either 10 ng/mL IL-4 and 10 ng/mL IL-13, or 50 ng/mL IFNγ and 100 ng/mL
876 LPS; or left unstimulated. RNA was collected at 6 hours post-synchronization, and qt-PCR was performed
877 to assess expression of genes encoding Arginase 1 (*Arg1*) and iNOS (*Nos2*). Shown are mean and
878 standard error of the mean (SEM), n=3 biological replicates. Statistical significance determined by
879 unpaired two-tailed T test with Welch's correction; *, $p < 0.05$; **, ***, $p<0.0005$. Data shown are
880 representative of 2 independent experiments.
881
882 **Supplemental Figure 2. The PER2-Luciferase reporter system enables real-time monitoring of circadian**
883 **rhythms of macrophages.** A schematic of the PER2-Luciferase (PER2-Luc) luciferase reporter system (A).
884 Bone marrow-derived macrophages (BMDMs) were derived from C57BL/6 mice expressing PER2-Luc.
885 The circadian clocks of BMDMs were synchronized by a 24-hour period of serum starvation in media with
886 0% serum, followed by a 2-hour period of serum shock in media with 50% serum. BMDMs were then
887 cultured in RPMI/10% FBS supplemented with D-luciferin, and luciferase activity was monitored in real
888 time by LumiCycle (B). Shown are mean and SEM; n=2 biological replicates. Data shown are
889 representative of 2 independent experiments.
890
891 **Supplemental Figure 3. Macrophages sense and respond to an acidic extracellular environment when**
892 **cultured *in vitro* in media with acidic pH.** Bone marrow-derived macrophages (BMDMs) were obtained
893 from C57BL/6 mice expressing PER2-Luc. BMDMs were cultured in media with pH 7.4 or acidic media
894 with pH 6.5, and stimulated with either 10 ng/mL IL-4 and 10 ng/mL IL-13, or 50 ng/mL IFNγ and 100

895 ng/mL LPS; or left unstimulated. RNA was collected at 2 hours post-treatment, and qt-PCR was
896 performed to assess expression of genes associated with phenotype (A) or acid sensing (B) in
897 macrophages. Shown are mean and SEM, n=3 biological replicates. Statistical significance determined by
898 two-tailed T test with Welch's correction; *, $p < 0.05$; **, $p<0.005$; ***, $p<0.0005$; ****, $p<0.00005$. Data
899 shown are representative of 2 independent experiments.
900
901 **Supplementary Figure 4. Survival of macrophages under acidic pH.** Bone marrow-derived macrophages
902 (BMDMs) were obtained from C57BL/6 mice expressing PER2-Luc. The circadian clocks of BMDMs were
903 synchronized by a 24-hour period of serum starvation in media with 0% serum, followed by a 2-hour
904 period of serum shock in media with 50% serum. BMDMs were then cultured in media with pH 7.4 or
905 acidic media with pH 6.8 or 6.5, and stimulated with either 10 ng/mL IL-4 and 10 ng/mL IL-13, or 50
906 ng/mL IFNγ and 100 ng/mL LPS; or left unstimulated. Cells were fixed at 1, 2, and 3 days post-treatment
907 and stained with DAPI. Number of nuclei was counted using Celigo to determine the number of adherent
908 cells. Shown are mean and SEM, n=3 biological replicates. Statistical significance determined by multiple
909 unpaired T test with Welch's correction; *, $p < 0.05$; **, $p<0.005$; ***, $p<0.0005$. Data shown are
910 representative of 2 independent experiments.
911
912 **Supplementary Figure 5. Pre-treatment with 15 uM MDL-12 for up to 2 hours is not necessary to**
913 **suppress pH-driven changes in amplitude of circadian rhythms.** Bone marrow-derived macrophages
914 (BMDMs) were obtained from C57BL/6 mice expressing PER2-Luc. The circadian clocks of BMDMs were
915 synchronized by a 24-hour period of serum starvation in media with 0% serum, followed by a 2-hour
916 period of serum shock in media with 50% serum. BMDMs were then cultured in media with neutral pH
917 7.4 or acidic pH 6.5, and treated with vehicle or 15uM MDL-12 (A). Alternately, BMDMs were cultured at
918 pH 7.4 and pre-treated with 15uM MDL-12 for 30 minutes (B, C) or 2 hours (D, E), after which media was

919 removed and cells were cultured in media at pH 7.4 or pH 6.5 in the presence (C, E) or absence (B, D) of
920 MDL-12. Luciferase activity was monitored in real time by LumiCycle. Shown is the mean, n=2 biological
921 replicates. Data for cells that received no pre-treatment (A) was overlaid on plots of data where cells
922 received pre-treatment (B-E) to allow for comparison of changes in rhythms.
923
924 **Supplementary Figure 6. Macrophages from BMAL1 KO mice have disrupted circadian rhythms.** Levels
925 of BMAL1 in bone marrow-derived macrophages (BMDMs) from WT or BMAL1 KO mice were assessed
926 by western blot (A). To confirm functional disruption of the circadian clock, peritoneal macrophages or
927 BMDMs were obtained from WT or BMAL1 KO mice expressing PER2-Luc and cultured in vitro with D-
928 luciferin. Luciferase activity was monitored in real time by LumiCycle (B). Shown is the mean and SEM,
929 n=2, representative of 2 independent experiments.

930 # References

931

932 1. Cassetta, L. and J.W. Pollard, *Targeting macrophages: therapeutic approaches in cancer.* Nat Rev
933 Drug Discov, 2018. **17**(12): p. 887-904.
934 2. Zhang, Q.W., et al., *Prognostic significance of tumor-associated macrophages in solid tumor: a*
935 *meta-analysis of the literature.* PLoS One, 2012. **7**(12): p. e50946.
936 3. Gentles, A.J., et al., *The prognostic landscape of genes and infiltrating immune cells across*
937 *human cancers.* Nat Med, 2015. **21**(8): p. 938-945.
938 4. DeNardo, D.G. and B. Ruffell, *Macrophages as regulators of tumour immunity and*
939 *immunotherapy.* Nat Rev Immunol, 2019.
940 5. Mosser, D.M. and J.P. Edwards, *Exploring the full spectrum of macrophage activation.* Nat Rev
941 Immunol, 2008. **8**(12): p. 958-69.
942 6. Murray, P.J. and T.A. Wynn, *Protective and pathogenic functions of macrophage subsets.* Nat Rev
943 Immunol, 2011. **11**(11): p. 723-37.
944 7. Coussens, L.M. and Z. Werb, *Inflammation and cancer.* Nature, 2002. **420**(6917): p. 860-7.
945 8. Murray, P.J., *Nonresolving macrophage-mediated inflammation in malignancy.* Febs j, 2018.
946 **285**(4): p. 641-653.
947 9. Schoppmann, S.F., et al., *Tumor-associated macrophages express lymphatic endothelial growth*
948 *factors and are related to peritumoral lymphangiogenesis.* Am J Pathol, 2002. **161**(3): p. 947-56.
949 10. Huber, R., et al., *Tumour hypoxia promotes melanoma growth and metastasis via High Mobility*
950 *Group Box-1 and M2-like macrophages.* Sci Rep, 2016. **6**: p. 29914.
951 11. Graham, D.K., et al., *The TAM family: phosphatidylserine sensing receptor tyrosine kinases gone*
952 *awry in cancer.* Nat Rev Cancer, 2014. **14**(12): p. 769-85.
953 12. Cook, R.S., et al., *MerTK inhibition in tumor leukocytes decreases tumor growth and metastasis.* J
954 Clin Invest, 2013. **123**(8): p. 3231-42.
955 13. Roberts, A.W., et al., *Tissue-Resident Macrophages Are Locally Programmed for Silent Clearance*
956 *of Apoptotic Cells.* Immunity, 2017. **47**(5): p. 913-927.e6.
957 14. Fadok, V.A., et al., *Macrophages that have ingested apoptotic cells in vitro inhibit*
958 *proinflammatory cytokine production through autocrine/paracrine mechanisms involving TGF-*
959 *beta, PGE2, and PAF.* J Clin Invest, 1998. **101**(4): p. 890-8.
960 15. Strassmann, G., et al., *Evidence for the involvement of interleukin 10 in the differential*
961 *deactivation of murine peritoneal macrophages by prostaglandin E2.* J Exp Med, 1994. **180**(6): p.
962 2365-70.
963 16. Kuang, D.M., et al., *Activated monocytes in peritumoral stroma of hepatocellular carcinoma*
964 *foster immune privilege and disease progression through PD-L1.* J Exp Med, 2009. **206**(6): p.
965 1327-37.
966 17. Ruffell, B. and L.M. Coussens, *Macrophages and therapeutic resistance in cancer.* Cancer Cell,
967 2015. **27**(4): p. 462-72.
968 18. Mantovani, A., et al., *Macrophages as tools and targets in cancer therapy.* Nature Reviews Drug
969 Discovery, 2022. **21**(11): p. 799-820.
970 19. Cuccarese, M.F., et al., *Heterogeneity of macrophage infiltration and therapeutic response in*
971 *lung carcinoma revealed by 3D organ imaging.* Nat Commun, 2017. **8**: p. 14293.
972 20. Chevrier, S., et al., *An Immune Atlas of Clear Cell Renal Cell Carcinoma.* Cell, 2017. **169**(4): p. 736-
973 749.e18.

21. Laviron, M., et al., *Tumor-associated macrophage heterogeneity is driven by tissue territories in breast cancer.* Cell Rep, 2022. **39**(8): p. 110865.
22. Nalio Ramos, R., et al., *Tissue-resident FOLR2(+) macrophages associate with CD8(+) T cell infiltration in human breast cancer.* Cell, 2022. **185**(7): p. 1189-1207.e25.
23. Yano, S., et al., *Spatial-temporal FUCCI imaging of each cell in a tumor demonstrates locational dependence of cell cycle dynamics and chemoresponsiveness.* Cell Cycle, 2014. **13**(13): p. 2110-9.
24. Huang, Y.K., et al., *Macrophage spatial heterogeneity in gastric cancer defined by multiplex immunohistochemistry.* Nat Commun, 2019. **10**(1): p. 3928.
25. Lyssiotis, C.A. and A.C. Kimmelman, *Metabolic Interactions in the Tumor Microenvironment.* Trends Cell Biol, 2017. **27**(11): p. 863-875.
26. Raghunand, N., R.A. Gatenby, and R.J. Gillies, *Microenvironmental and cellular consequences of altered blood flow in tumours.* Br J Radiol, 2003. **76 Spec No 1**: p. S11-22.
27. Gillies, R.J., et al., *Targeting acidity in cancer and diabetes.* Biochim Biophys Acta Rev Cancer, 2019. **1871**(2): p. 273-280.
28. El-Kenawi, A., et al., *Acidity promotes tumour progression by altering macrophage phenotype in prostate cancer.* Br J Cancer, 2019. **121**(7): p. 556-566.
29. Bohn, T., et al., *Tumor immunoevasion via acidosis-dependent induction of regulatory tumor-associated macrophages.* Nat Immunol, 2018. **19**(12): p. 1319-1329.
30. Jiang, W., et al., *Extracellular Acidity Reprograms Macrophage Metabolism and Innate Responsiveness.* The Journal of Immunology, 2021. **206**(12): p. 3021-3031.
31. Partch, C.L., C.B. Green, and J.S. Takahashi, *Molecular architecture of the mammalian circadian clock.* Trends Cell Biol, 2014. **24**(2): p. 90-9.
32. Walton, Z.E., et al., *Acid Suspends the Circadian Clock in Hypoxia through Inhibition of mTOR.* Cell, 2018. **174**(1): p. 72-87.e32.
33. Mure, L.S., et al., *Diurnal transcriptome atlas of a primate across major neural and peripheral tissues.* Science, 2018. **359**(6381).
34. Zhang, R., et al., *A circadian gene expression atlas in mammals: implications for biology and medicine.* Proc Natl Acad Sci U S A, 2014. **111**(45): p. 16219-24.
35. Haspel, J.A., et al., *Perfect timing: circadian rhythms, sleep, and immunity - an NIH workshop summary.* JCI Insight, 2020. **5**(1).
36. Keller, M., et al., *A circadian clock in macrophages controls inflammatory immune responses.* Proc Natl Acad Sci U S A, 2009. **106**(50): p. 21407-12.
37. Silver, A.C., et al., *Circadian expression of clock genes in mouse macrophages, dendritic cells, and B cells.* Brain Behav Immun, 2012. **26**(3): p. 407-13.
38. Nguyen, K.D., et al., *Circadian gene Bmal1 regulates diurnal oscillations of Ly6C(hi) inflammatory monocytes.* Science, 2013. **341**(6153): p. 1483-8.
39. Baumann, A., et al., *The circadian clock is functional in eosinophils and mast cells.* Immunology, 2013. **140**(4): p. 465-74.
40. Adrover, J.M., et al., *A Neutrophil Timer Coordinates Immune Defense and Vascular Protection.* Immunity, 2019. **50**(2): p. 390-402.e10.
41. Arjona, A. and D.K. Sarkar, *Circadian oscillations of clock genes, cytolytic factors, and cytokines in rat NK cells.* J Immunol, 2005. **174**(12): p. 7618-24.
42. Druzd, D., et al., *Lymphocyte Circadian Clocks Control Lymph Node Trafficking and Adaptive Immune Responses.* Immunity, 2017. **46**(1): p. 120-132.
43. Scheiermann, C., et al., *Clocking in to immunity.* Nat Rev Immunol, 2018. **18**(7): p. 423-437.
44. Kitchen, G.B., et al., *The clock gene Bmal1 inhibits macrophage motility, phagocytosis, and impairs defense against pneumonia.* Proc Natl Acad Sci U S A, 2020.

1021 45. Gibbs, J.E., et al., *The nuclear receptor REV-ERBalpha mediates circadian regulation of innate*
1022 *immunity through selective regulation of inflammatory cytokines.* Proc Natl Acad Sci U S A, 2012.
1023 **109**(2): p. 582-7.
1024 46. He, W., et al., *Circadian Expression of Migratory Factors Establishes Lineage-Specific Signatures*
1025 *that Guide the Homing of Leukocyte Subsets to Tissues.* Immunity, 2018. **49**(6): p. 1175-1190.e7.
1026 47. Nobis, C.C., et al., *The circadian clock of CD8 T cells modulates their early response to vaccination*
1027 *and the rhythmicity of related signaling pathways.* Proc Natl Acad Sci U S A, 2019. **116**(40): p.
1028 20077-20086.
1029 48. Fortier, E.E., et al., *Circadian variation of the response of T cells to antigen.* J Immunol, 2011.
1030 **187**(12): p. 6291-300.
1031 49. Beam, C.A., et al., *Synchronization of the Normal Human Peripheral Immune System: A*
1032 *Comprehensive Circadian Systems Immunology Analysis.* Sci Rep, 2020. **10**(1): p. 672.
1033 50. Mazzoccoli, G., et al., *A timetable of 24-hour patterns for human lymphocyte subpopulations.* J
1034 Biol Regul Homeost Agents, 2011. **25**(3): p. 387-95.
1035 51. Silver, A.C., et al., *The circadian clock controls toll-like receptor 9-mediated innate and adaptive*
1036 *immunity.* Immunity, 2012. **36**(2): p. 251-61.
1037 52. Phillips, A.C., et al., *Preliminary evidence that morning vaccination is associated with an*
1038 *enhanced antibody response in men.* Psychophysiology, 2008. **45**(4): p. 663-6.
1039 53. Long, J.E., et al., *Morning vaccination enhances antibody response over afternoon vaccination: A*
1040 *cluster-randomised trial.* Vaccine, 2016. **34**(24): p. 2679-85.
1041 54. Curtis, A.M., et al., *Circadian control of innate immunity in macrophages by miR-155 targeting*
1042 *Bmal1.* Proc Natl Acad Sci U S A, 2015. **112**(23): p. 7231-6.
1043 55. Deng, W., et al., *The Circadian Clock Controls Immune Checkpoint Pathway in Sepsis.* Cell Rep,
1044 2018. **24**(2): p. 366-378.
1045 56. Aiello, I., et al., *Circadian disruption promotes tumor-immune microenvironment remodeling*
1046 *favoring tumor cell proliferation.* Sci Adv, 2020. **6**(42).
1047 57. Tsuruta, A., et al., *Diurnal Expression of PD-1 on Tumor-Associated Macrophages Underlies the*
1048 *Dosing Time-Dependent Antitumor Effects of the PD-1/PD-L1 Inhibitor BMS-1 in B16/BL6*
1049 *Melanoma-Bearing Mice.* Mol Cancer Res, 2022. **20**(6): p. 972-982.
1050 58. Strauss, L., et al., *Targeted deletion of PD-1 in myeloid cells induces antitumor immunity.* Sci
1051 Immunol, 2020. **5**(43).
1052 59. Qian, D.C., et al., *Effect of immunotherapy time-of-day infusion on overall survival among*
1053 *patients with advanced melanoma in the USA (MEMOIR): a propensity score-matched analysis of*
1054 *a single-centre, longitudinal study.* Lancet Oncol, 2021. **22**(12): p. 1777-1786.
1055 60. Martinez, F.O. and S. Gordon, *The M1 and M2 paradigm of macrophage activation: time for*
1056 *reassessment.* F1000Prime Rep, 2014. **6**: p. 13.
1057 61. Yoo, S.H., et al., *PERIOD2::LUCIFERASE real-time reporting of circadian dynamics reveals*
1058 *persistent circadian oscillations in mouse peripheral tissues.* Proc Natl Acad Sci U S A, 2004.
1059 **101**(15): p. 5339-46.
1060 62. Rodheim, K., C. Jung, and K. Wright, *016 Associations between Circadian Melatonin and*
1061 *Temperature Amplitudes during Constant Routine.* Sleep, 2021. **44**(Supplement_2): p. A8-A8.
1062 63. Wu, G., et al., *Normalized coefficient of variation (nCV): a method to evaluate circadian clock*
1063 *robustness in population scale data.* Bioinformatics, 2021. **37**(23): p. 4581-4583.
1064 64. Chen, S., et al., *A Pro- and Anti-inflammatory Axis Modulates the Macrophage Circadian Clock.*
1065 Front Immunol, 2020. **11**: p. 867.
1066 65. Lellupitiyage Don, S.S., et al., *Macrophage circadian rhythms are differentially affected based on*
1067 *stimuli.* Integr Biol (Camb), 2022. **14**(3): p. 62-75.

1068 66. Pilorz, V., et al., *A Novel Mechanism Controlling Resetting Speed of the Circadian Clock to*
1069 *Environmental Stimuli.* Current Biology, 2014. **24**(7): p. 766-773.
1070 67. Abe, M., et al., *Circadian rhythms in isolated brain regions.* J Neurosci, 2002. **22**(1): p. 350-6.
1071 68. Gaspar, L.S., et al., *The importance of determining circadian parameters in pharmacological*
1072 *studies.* British Journal of Pharmacology, 2019. **176**(16): p. 2827-2847.
1073 69. Boedtkjer, E. and S.F. Pedersen, *The Acidic Tumor Microenvironment as a Driver of Cancer.*
1074 Annual Review of Physiology, 2020. **82**(1): p. 103-126.
1075 70. Gillies, R.J., Z. Liu, and Z. Bhujwalla, *31P-MRS measurements of extracellular pH of tumors using*
1076 *3-aminopropylphosphonate.* Am J Physiol, 1994. **267**(1 Pt 1): p. C195-203.
1077 71. Estrella, V., et al., *Acidity Generated by the Tumor Microenvironment Drives Local Invasion.*
1078 Cancer Research, 2013. **73**(5): p. 1524-1535.
1079 72. Lv, S., et al., *A negative feedback loop of ICER and NF-κB regulates TLR signaling in innate*
1080 *immune responses.* Cell Death Differ, 2017. **24**(3): p. 492-499.
1081 73. Kraut, J.A. and N.E. Madias, *Lactic acidosis.* N Engl J Med, 2014. **371**(24): p. 2309-19.
1082 74. Pastorekova, S. and R.J. Gillies, *The role of carbonic anhydrase IX in cancer development: links to*
1083 *hypoxia, acidosis, and beyond.* Cancer Metastasis Rev, 2019. **38**(1-2): p. 65-77.
1084 75. Swietach, P., *What is pH regulation, and why do cancer cells need it?* Cancer Metastasis Rev,
1085 2019. **38**(1-2): p. 5-15.
1086 76. de la Cruz-López, K.G., et al., *Lactate in the Regulation of Tumor Microenvironment and*
1087 *Therapeutic Approaches.* Front Oncol, 2019. **9**: p. 1143.
1088 77. Colegio, O.R., et al., *Functional polarization of tumour-associated macrophages by tumour-*
1089 *derived lactic acid.* Nature, 2014. **513**(7519): p. 559-63.
1090 78. Polumuri, S., D.J. Perkins, and S.N. Vogel, *cAMP levels regulate macrophage alternative*
1091 *activation marker expression.* Innate Immun, 2021. **27**(2): p. 133-142.
1092 79. Tavares, L.P., et al., *Blame the signaling: Role of cAMP for the resolution of inflammation.*
1093 Pharmacol Res, 2020. **159**: p. 105030.
1094 80. Yagita, K. and H. Okamura, *Forskolin induces circadian gene expression of rPer1, rPer2 and dbp in*
1095 *mammalian rat-1 fibroblasts.* FEBS Lett, 2000. **465**(1): p. 79-82.
1096 81. O'Neill, J.S., et al., *cAMP-dependent signaling as a core component of the mammalian circadian*
1097 *pacemaker.* Science, 2008. **320**(5878): p. 949-53.
1098 82. Misra, U.K. and S.V. Pizzo, *Coordinate regulation of forskolin-induced cellular proliferation in*
1099 *macrophages by protein kinase A/cAMP-response element-binding protein (CREB) and Epac1-*
1100 *Rap1 signaling: effects of silencing CREB gene expression on Akt activation.* J Biol Chem, 2005.
1101 **280**(46): p. 38276-89.
1102 83. Geeraerts, X., et al., *Macrophage Metabolism As Therapeutic Target for Cancer, Atherosclerosis,*
1103 *and Obesity.* Front Immunol, 2017. **8**: p. 289.
1104 84. Shilts, J., G. Chen, and J.J. Hughey, *Evidence for widespread dysregulation of circadian clock*
1105 *progression in human cancer.* PeerJ, 2018. **6**: p. e4327.
1106 85. Pariollaud, M., et al., *Circadian disruption enhances HSF1 signaling and tumorigenesis in Kras-*
1107 *driven lung cancer.* Science Advances, 2022. **8**(39): p. eabo1123.
1108 86. Besmer, D.M., et al., *Pancreatic ductal adenocarcinoma mice lacking mucin 1 have a profound*
1109 *defect in tumor growth and metastasis.* Cancer Res, 2011. **71**(13): p. 4432-42.
1110 87. Kidiyoor, A., et al., *Pancreatic Cancer Cells Isolated from Muc1-Null Tumors Favor the Generation*
1111 *of a Mature Less Suppressive MDSC Population.* Front Immunol, 2014. **5**: p. 67.
1112 88. Alexander, R.K., et al., *Bmal1 integrates mitochondrial metabolism and macrophage activation.*
1113 eLife, 2020. **9**: p. e54090.
1114 89. Lee, C.-C., et al., *Macrophage-secreted interleukin-35 regulates cancer cell plasticity to facilitate*
1115 *metastatic colonization.* Nature Communications, 2018. **9**(1): p. 3763.

1116 90. Walton, Z.E., R.C. Brooks, and C.V. Dang, *mTOR Senses Intracellular pH through Lysosome*
1117 *Dispersion from RHEB.* Bioessays, 2019: p. e1800265.
1118 91. Guellaen, G., et al., *RMI 12330 A, an inhibitor of adenylate cyclase in rat liver.* Biochim Biophys
1119 Acta, 1977. **484**(2): p. 465-75.
1120 92. Hunt, N.H. and T. Evans, *RMI 12330A, an inhibitor of cyclic nucleotide phosphodiesterases and*
1121 *adenylate cyclase in kidney preparations.* Biochim Biophys Acta, 1980. **613**(2): p. 499-506.
1122 93. van Rossum, D.B., et al., *Ca2+ entry mediated by store depletion, S-nitrosylation, and TRP3*
1123 *channels. Comparison of coupling and function.* J Biol Chem, 2000. **275**(37): p. 28562-8.
1124 94. O'Neill, J.S. and A.B. Reddy, *The essential role of cAMP/Ca2+ signalling in mammalian circadian*
1125 *timekeeping.* Biochem Soc Trans, 2012. **40**(1): p. 44-50.
1126 95. Ni, L., et al., *Identification and Function of Acid-sensing Ion Channels in RAW 264.7 Macrophage*
1127 *Cells.* Curr Med Sci, 2018. **38**(3): p. 436-442.
1128 96. Selezneva, A., A.J. Gibb, and D. Willis, *The contribution of ion channels to shaping macrophage*
1129 *behaviour.* Front Pharmacol, 2022. **13**: p. 970234.
1130 97. Putker, M., et al., *Mammalian Circadian Period, But Not Phase and Amplitude, Is Robust Against*
1131 *Redox and Metabolic Perturbations.* Antioxidants & Redox Signaling, 2017. **28**(7): p. 507-520.
1132 98. Viola, A., et al., *The Metabolic Signature of Macrophage Responses.* Front Immunol, 2019. **10**: p.
1133 1462.
1134 99. Morris, E.L., et al., *Single-cell transcriptomics of suprachiasmatic nuclei reveal a Prokineticin-*
1135 *driven circadian network.* Embo j, 2021. **40**(20): p. e108614.
1136 100. Ma, D., et al., *A transcriptomic taxonomy of Drosophila circadian neurons around the clock.* Elife,
1137 2021. **10**.
1138 101. Auerbach, B.J., G.A. FitzGerald, and M. Li, *Tempo: an unsupervised Bayesian algorithm for*
1139 *circadian phase inference in single-cell transcriptomics.* Nat Commun, 2022. **13**(1): p. 6580.
1140 102. Finger, A.M., et al., *Intercellular coupling between peripheral circadian oscillators by TGF-β*
1141 *signaling.* Sci Adv, 2021. **7**(30).
1142 103. Massagué, J., *TGFb in Cancer.* Cell, 2008. **134**(2): p. 215-230.
1143 104. Geiger, S.S., et al., *Daily variation in macrophage phagocytosis is clock-independent and*
1144 *dispensable for cytokine production.* Immunology, 2019.
1145 105. Ramanathan, C., et al., *Cell Type-Specific Functions of Period Genes Revealed by Novel Adipocyte*
1146 *and Hepatocyte Circadian Clock Models.* PLOS Genetics, 2014. **10**(4): p. e1004244.
1147 106. Committee, N.R.C., *Guide for the Care and Use of Laboratory Animals*, in *Guide for the Care and*
1148 *Use of Laboratory Animals*. 2011, National Academies Press (US)
1149 Copyright © 2011, National Academy of Sciences.: Washington (DC).
1150 107. Clausen, B.E., et al., *Conditional gene targeting in macrophages and granulocytes using LysMcre*
1151 *mice.* Transgenic Res, 1999. **8**(4): p. 265-77.
1152 108. Storch, K.F., et al., *Intrinsic circadian clock of the mammalian retina: importance for retinal*
1153 *processing of visual information.* Cell, 2007. **130**(4): p. 730-741.
1154 109. Trouplin, V., et al., *Bone marrow-derived macrophage production.* J Vis Exp, 2013(81): p. e50966.
1155 110. Gonçalves, R. and D.M. Mosser, *The Isolation and Characterization of Murine Macrophages.*
1156 Current Protocols in Immunology, 2015. **111**(1): p. 14.1.1-14.1.16.
1157 111. Ray, A. and B.N. Dittel, *Isolation of mouse peritoneal cavity cells.* J Vis Exp, 2010(35).
1158 112. Liu, P.S., et al., *alpha-ketoglutarate orchestrates macrophage activation through metabolic and*
1159 *epigenetic reprogramming.* Nat Immunol, 2017. **18**(9): p. 985-994.
1160 113. Huber, A.L., et al., *CRY2 and FBXL3 Cooperatively Degrade c-MYC.* Mol Cell, 2016. **64**(4): p. 774-
1161 789.
1162 114. Tomayko, M.M. and C.P. Reynolds, *Determination of subcutaneous tumor size in athymic (nude)*
1163 *mice.* Cancer Chemother Pharmacol, 1989. **24**(3): p. 148-54.

1164 115. Patro, R., et al., *Salmon provides fast and bias-aware quantification of transcript expression.* Nat
1165 Methods, 2017. **14**(4): p. 417-419.
1166 116. Soneson, C., M.I. Love, and M.D. Robinson, *Differential analyses for RNA-seq: transcript-level*
1167 *estimates improve gene-level inferences.* F1000Res, 2015. **4**: p. 1521.
1168 117. Ritchie, M.E., et al., *limma powers differential expression analyses for RNA-sequencing and*
1169 *microarray studies.* Nucleic Acids Res, 2015. **43**(7): p. e47.
1170 118. Dai, M., et al., *Evolving gene/transcript definitions significantly alter the interpretation of*
1171 *GeneChip data.* Nucleic Acids Res, 2005. **33**(20): p. e175.
1172

Fig 1

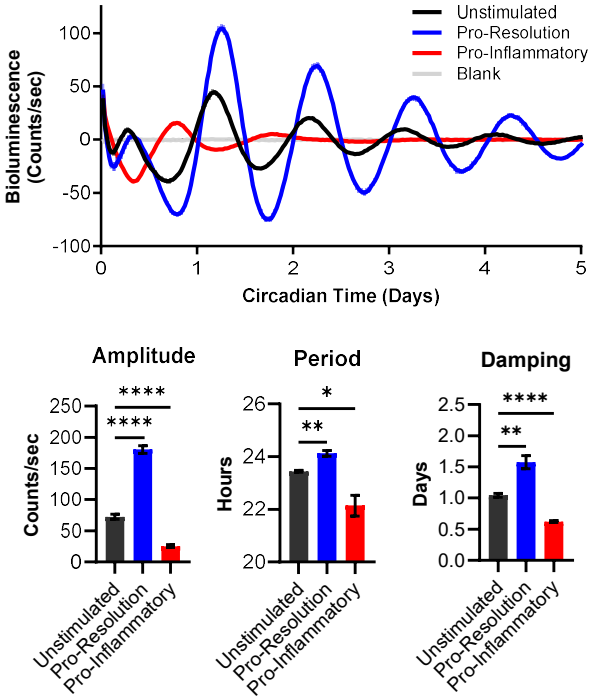
Unstimulated
Pro-Resolution
Pro-Inflammatory
Blank
Bioluminescence (Counts/sec)
100
50
0
-50
-100
0
1
2
3
4
5
Circadian Time (Days)
Amplitude
Period
Damping
Counts/sec
Hours
Days
****
****
*
**
****
**
Unstimulated
Pro-Resolution
Pro-Inflammatory

Fig 2

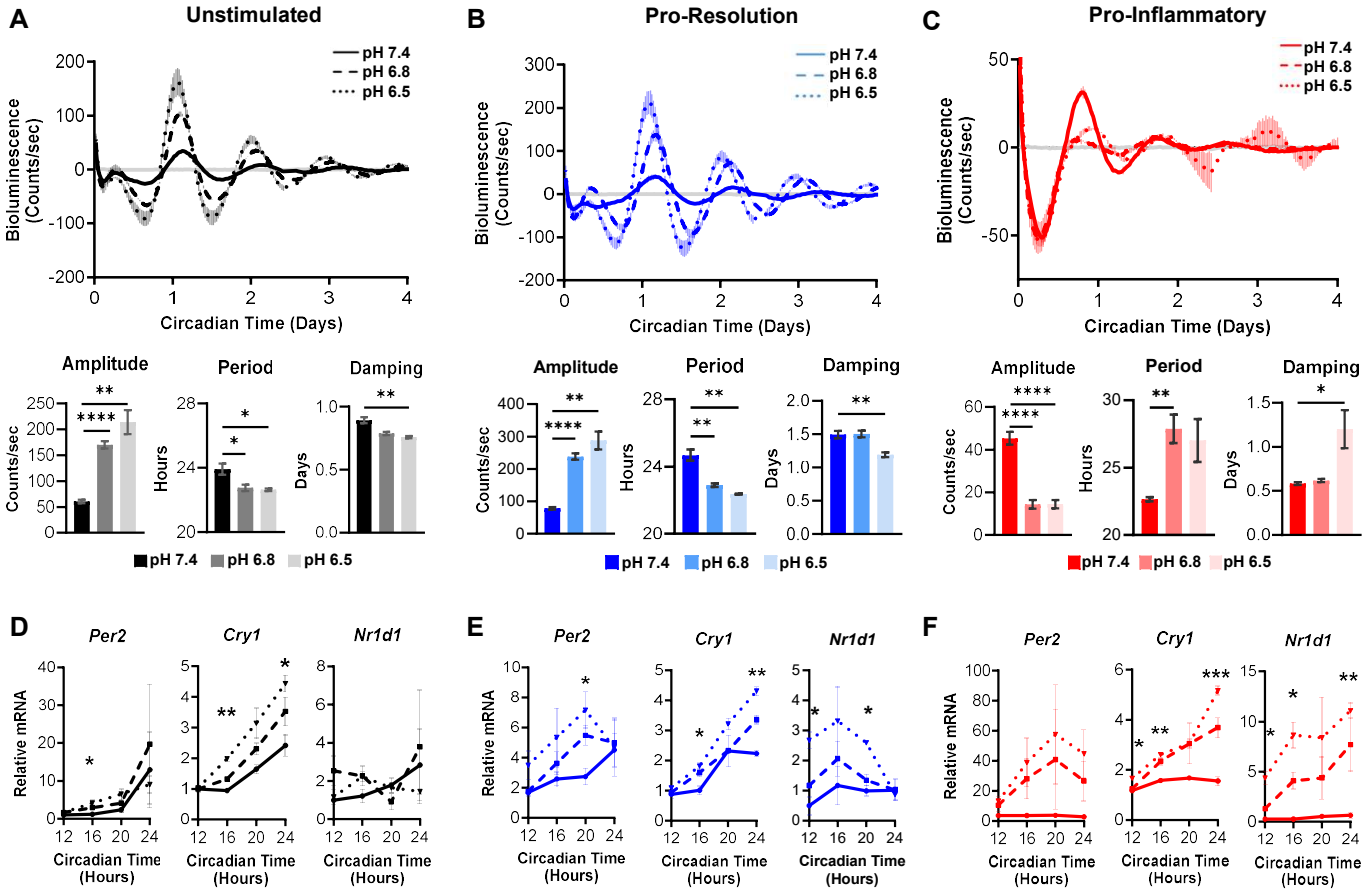
A
Unstimulated
pH 7.4
pH 6.8
pH 6.5
Bioluminescence (Counts/sec)
Circadian Time (Days)
Amplitude
Period
Damping
Counts/sec
Hours
Days
B
Pro-Resolution
C
Pro-Inflammatory
D
Per2
Cry1
Nr1d1
Relative mRNA
Circadian Time (Hours)
E
F

Fig 3

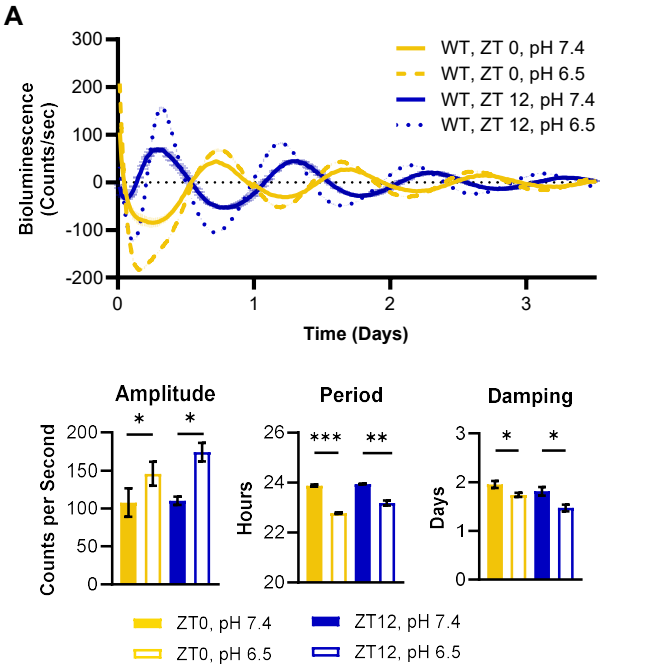
A
Bioluminescence (Counts/sec)
300
200
100
0
-100
-200
0
1
2
3
Time (Days)
WT, ZT 0, pH 7.4
WT, ZT 0, pH 6.5
WT, ZT 12, pH 7.4
WT, ZT 12, pH 6.5
Amplitude
Period
Damping
Counts per Second
Hours
Days
*
*
***
**
*
*
ZT0, pH 7.4
ZT0, pH 6.5
ZT12, pH 7.4
ZT12, pH 6.5

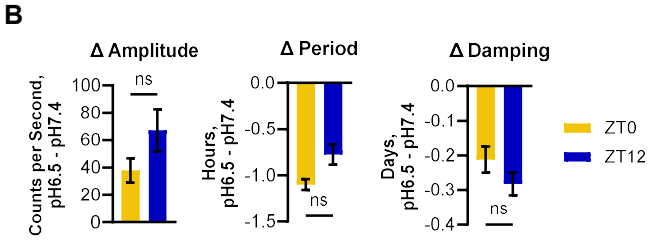
B
Δ Amplitude
Δ Period
Δ Damping
Counts per Second, pH6.5 - pH7.4
Hours, pH6.5 - pH7.4
Days, pH6.5 - pH7.4
ns
ns
ns
ZT0
ZT12

Fig 4

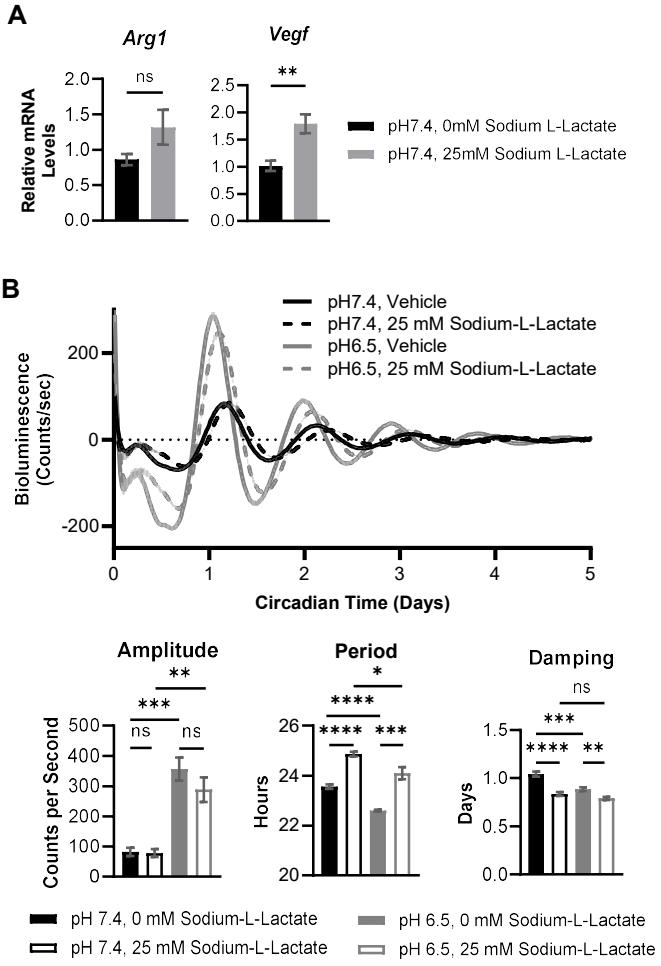
A
Arg1
Vegf
Relative mRNA Levels
ns
**
pH7.4, 0mM Sodium L-Lactate
pH7.4, 25mM Sodium L-Lactate
B
pH7.4, Vehicle
pH7.4, 25 mM Sodium-L-Lactate
pH6.5, Vehicle
pH6.5, 25 mM Sodium-L-Lactate
Bioluminescence (Counts/sec)
Circadian Time (Days)
Amplitude
Period
Damping
Counts per Second
Hours
Days
pH 7.4, 0 mM Sodium-L-Lactate
pH 7.4, 25 mM Sodium-L-Lactate
pH 6.5, 0 mM Sodium-L-Lactate
pH 6.5, 25 mM Sodium-L-Lactate

Fig 5

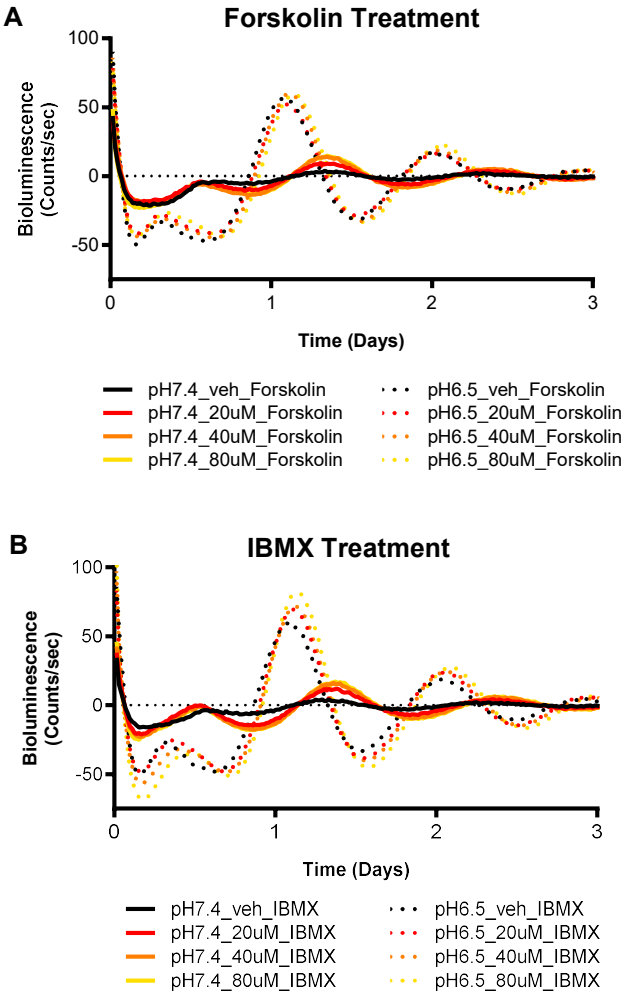
A
Forskolin Treatment
Bioluminescence (Counts/sec)
100
50
0
-50
0
1
2
3
Time (Days)
pH7.4_veh_Forskolin
pH7.4_20uM_Forskolin
pH7.4_40uM_Forskolin
pH7.4_80uM_Forskolin
pH6.5_veh_Forskolin
pH6.5_20uM_Forskolin
pH6.5_40uM_Forskolin
pH6.5_80uM_Forskolin
B
IBMX Treatment
Bioluminescence (Counts/sec)
100
50
0
-50
0
1
2
3
Time (Days)
pH7.4_veh_IBMX
pH7.4_20uM_IBMX
pH7.4_40uM_IBMX
pH7.4_80uM_IBMX
pH6.5_veh_IBMX
pH6.5_20uM_IBMX
pH6.5_40uM_IBMX
pH6.5_80uM_IBMX

Fig 6

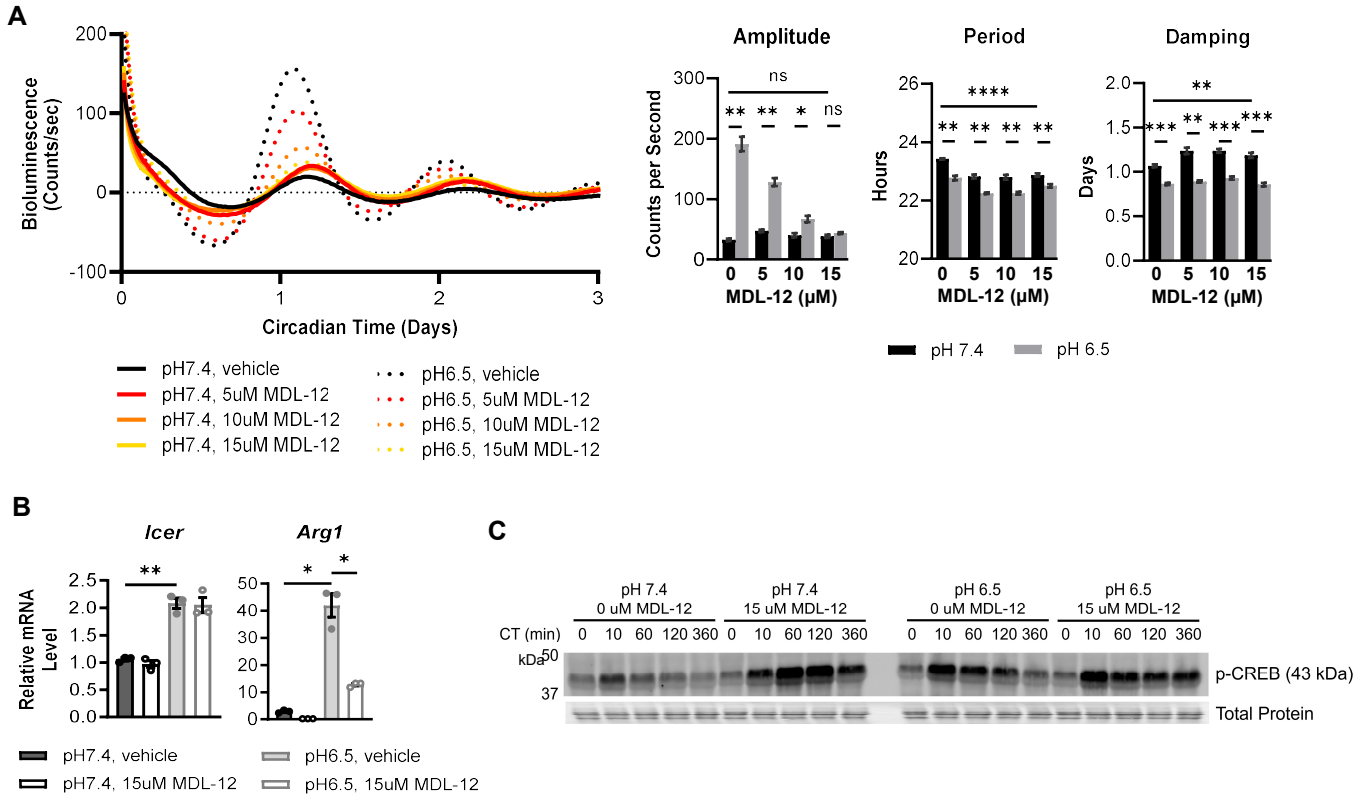
A
Bioluminescence (Counts/sec)
Circadian Time (Days)
pH7.4, vehicle
pH7.4, 5uM MDL-12
pH7.4, 10uM MDL-12
pH7.4, 15uM MDL-12
pH6.5, vehicle
pH6.5, 5uM MDL-12
pH6.5, 10uM MDL-12
pH6.5, 15uM MDL-12
Amplitude
Period
Damping
Counts per Second
Hours
Days
MDL-12 (μM)
ns
pH 7.4
pH 6.5

B
Icer
Arg1
Relative mRNA Level
pH7.4, vehicle
pH7.4, 15uM MDL-12
pH6.5, vehicle
pH6.5, 15uM MDL-12
C
pH 7.4
0 uM MDL-12
pH 7.4
15 uM MDL-12
pH 6.5
0 uM MDL-12
pH 6.5
15 uM MDL-12
CT (min)
kDa
p-CREB (43 kDa)
Total Protein

Fig 7

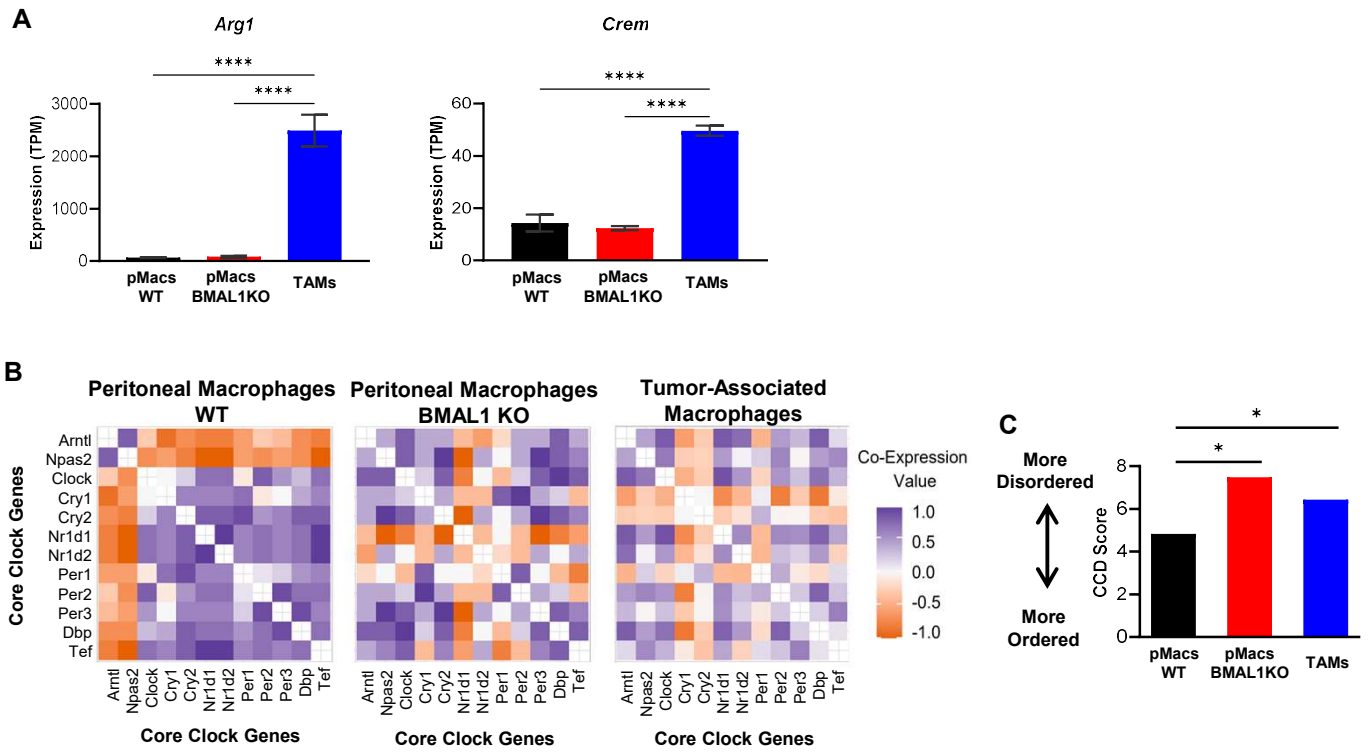
A
Arg1
Crem
****
Expression (TPM)
pMacs WT
pMacs BMAL1KO
TAMs
B
Peritoneal Macrophages WT
Peritoneal Macrophages BMAL1 KO
Tumor-Associated Macrophages
Core Clock Genes
Arntl
Npas2
Clock
Cry1
Cry2
Nr1d1
Nr1d2
Per1
Per2
Per3
Dbp
Tef
Co-Expression Value
1.0
0.5
0.0
-0.5
-1.0
C
More Disordered
More Ordered
CCD Score
*

Fig 8

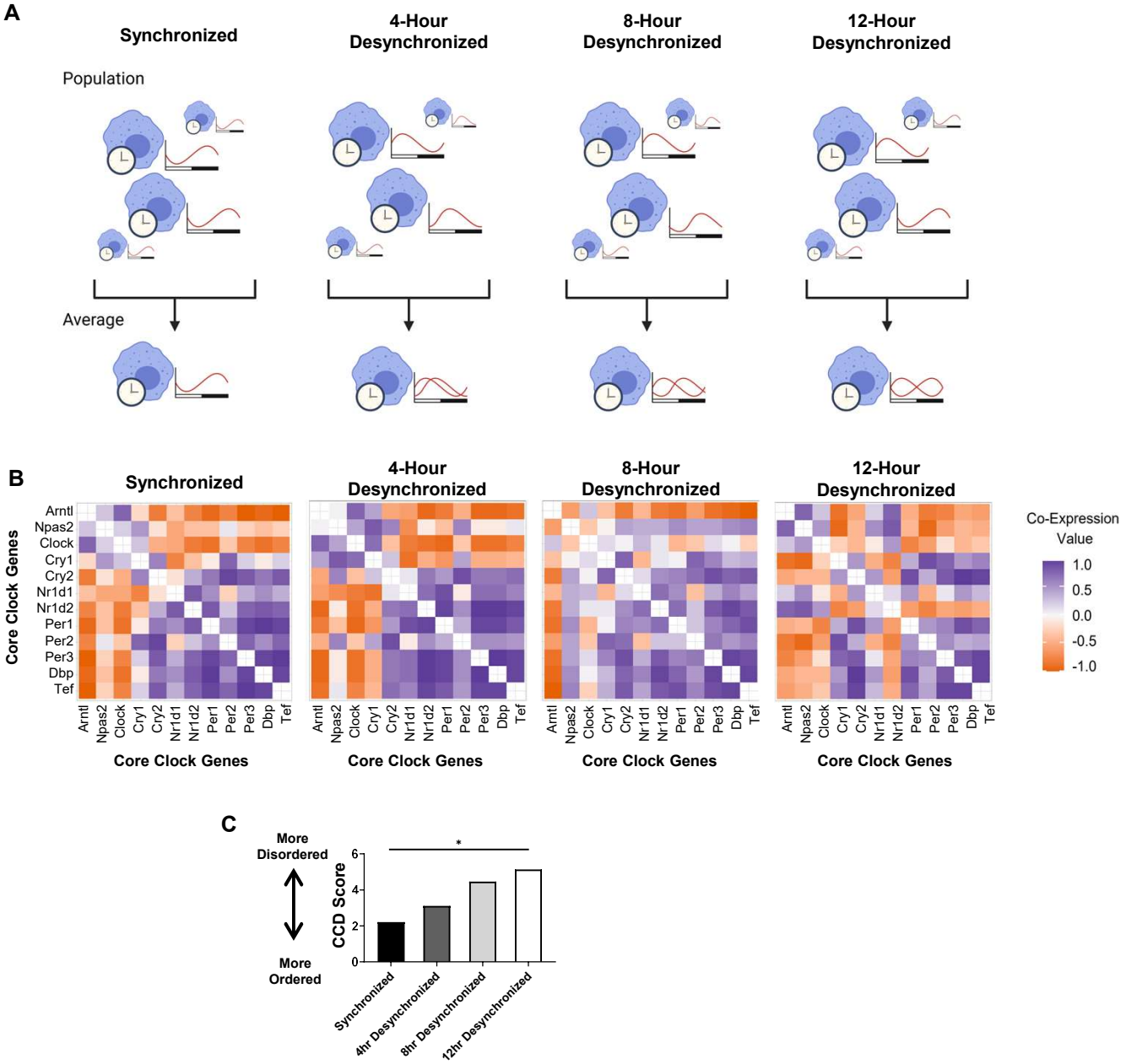
A
Synchronized
4-Hour Desynchronized
8-Hour Desynchronized
12-Hour Desynchronized
Population
Average
B
Synchronized
4-Hour Desynchronized
8-Hour Desynchronized
12-Hour Desynchronized
Core Clock Genes
Arntl
Npas2
Clock
Cry1
Cry2
Nr1d1
Nr1d2
Per1
Per2
Per3
Dbp
Tef
Co-Expression Value
1.0
0.5
0.0
-0.5
-1.0
C
More Disordered
More Ordered
CCD Score
0
2
4
6
*
Synchronized
4hr Desynchronized
8hr Desynchronized
12hr Desynchronized

Fig 9

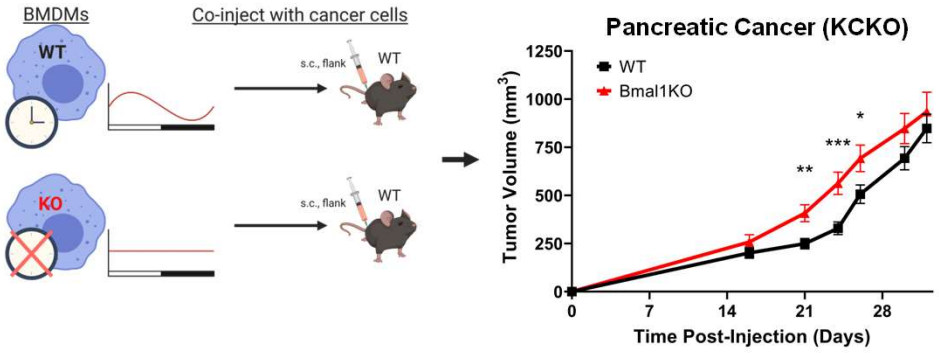
BMDMs
Co-inject with cancer cells
WT
KO
s.c., flank
WT
s.c., flank
WT
Pancreatic Cancer (KCKO)
WT
Bmal1KO
Tumor Volume (mm3)
1250
1000
750
500
250
0
**
***
*
0
7
14
21
28
Time Post-Injection (Days)